

# UNIVERSIDAD DE CONCEPCIÓN



## CENTRO DE INVESTIGACIÓN EN INGENIERÍA MATEMÁTICA (CI<sup>2</sup>MA)



**A posteriori error analysis of a momentum and thermal energy  
conservative mixed-FEM for the Boussinesq equations**

SERGIO CAUCAO, RICARDO OYARZÚA,  
SEGUNDO VILLA-FUENTES

PREPRINT 2020-29

SERIE DE PRE-PUBLICACIONES



# A posteriori error analysis of a momentum and thermal energy conservative mixed-FEM for the Boussinesq equations. \*

SERGIO CAUCAO<sup>†</sup> RICARDO OYARZÚA<sup>‡</sup> AND SEGUNDO VILLA-FUENTES<sup>§</sup>

## Abstract

In this paper we complement the study of a new mixed finite element scheme, allowing conservation of momentum and thermal energy, for the Boussinesq model describing natural convection and derive a reliable and efficient residual-based *a posteriori* error estimator for the corresponding Galerkin scheme in two and three dimensions. More precisely, by extending standard techniques commonly used on Hilbert spaces to the case of Banach spaces, such as local estimates, suitable Helmholtz decompositions and the local approximation properties of the Clément and Raviart–Thomas operators, we derive the aforementioned *a posteriori* error estimator on arbitrary (convex or non-convex) polygonal and polyhedral regions. In turn, inverse inequalities, the localization technique based on bubble functions, and known results from previous works, are employed to prove the local efficiency of the proposed *a posteriori* error estimator. Finally, to illustrate the performance of the adaptive algorithm based on the proposed *a posteriori* error indicator and to corroborate the theoretical results, we provide some numerical examples.

**Key words:** stationary Boussinesq equations, mixed finite element method, conservation of momentum, conservation of thermal energy, Banach spaces, Raviart-Thomas elements, a posteriori error estimator, reliability, local efficiency.

**Mathematics subject classifications (2000):** 65N30, 65N12, 65N15, 35Q79, 80A20, 76R05, 76D07

## 1 Introduction

The derivation of new finite element methods for the Boussinesq model describing natural convection, in which the steady-state equations of momentum (Navier-Stokes) and thermal energy are coupled by means of the so called Boussinesq approximation, has become a very active research area lately (see, e.g. [3, 2, 15, 16, 19, 18, 23, 32, 33, 34]). The above list includes Discontinuous Galerkin and stabilized methods, mixed and augmented-mixed approaches and generalizations of the Boussinesq model with temperature-dependent parameters.

---

\*This work was partially supported by CONICYT-Chile through project AFB170001 of the PIA Program: Concurso Apoyo a Centros Científicos y Tecnológicos de Excelencia con Financiamiento Basal, project Fondecyt 1161325, project PAI77190084 of the PAI Program: Convocatoria Nacional Subvención a la Instalación en la Academia, ANID BECAS/DOCTORADO NACIONAL 21180900; and by Universidad del Bío-Bío through VRIP-UBB project 194608 GI/C.

<sup>†</sup>Departamento de Matemática y Física Aplicadas, Universidad Católica de la Santísima Concepción, Casilla 297, Concepción, Chile, email: [scaucao@ucsc.cl](mailto:scaucao@ucsc.cl)

<sup>‡</sup>GIMNAP-Departamento de Matemática, Universidad del Bío-Bío, Casilla 5-C, Concepción, Chile, and CI<sup>2</sup>MA, Universidad de Concepción, Casilla 160-C, Concepción, Chile, email: [royarzua@ubiobio.cl](mailto:royarzua@ubiobio.cl).

<sup>§</sup>GIMNAP-Departamento de Matemática, Universidad del Bío-Bío, Casilla 5-C, Concepción, Chile, email: [segundo.villa1701@alumnos.ubiobio.cl](mailto:segundo.villa1701@alumnos.ubiobio.cl).

Now, in the recent paper [13] we have developed a new Banach spaces-based mixed finite element method for the Boussinesq problem which allows, on the one hand, to conserve momentum and thermal energy if the external forces belong to the velocity and temperature discrete spaces, respectively, and on the other hand, to compute further variables of interest, such as the fluid vorticity, the fluid velocity gradient, and the heat-flux, through a simple postprocess of the finite element solutions, in which no numerical differentiation is applied, and hence no further sources of error arise. More precisely, we introduce a modified pseudostress tensor depending on the pressure, and the diffusive and convective terms of the Navier–Stokes equations for the fluid, and a vector unknown involving the temperature, its gradient and the velocity, and derive a mixed variational formulation where the aforementioned pseudostress tensor and vector unknown, together with the velocity and the temperature, are the main unknowns of the system. In turn, the associated numerical scheme is defined by Raviart–Thomas elements of order  $k$  for the pseudostress tensor and the vector unknown, and discontinuous piece-wise polynomial elements of degree  $k$  for the velocity and temperature. With this choice of discrete spaces the proposed Galerkin scheme becomes well posed and optimal convergent.

The aim of the present work is to complement the study started in [13] by introducing a reliable and efficient residual-based *a posteriori* error estimator for the associated mixed scheme. In this direction, we mention that the first contribution dealing with adaptive algorithms for mixed formulations of the Boussinesq problem is [24] where the authors introduced appropriate refinement rules to recover the quasi-optimality of the method proposed in [23] under the presence of singular behaviors near non-convex corner points. More recently, in the contributions [20, 17] the authors proposed reliable and efficient *a posteriori* error estimators for augmented mixed-based formulations of the Boussinesq equations. In [20] the error indicator is non-local due to the presence of the  $H^{1/2}$ -norm of a residual term involving the temperature on the boundary, whereas in [17] the estimator turns to be fully-local and fully-computable. However, in both cases the efficiency estimate cannot be localized due to the presence of the convective term in some of the terms defining the error indicator. These works were extended in [6] to the case of natural convection models with temperature-dependent viscosity. Finally, for adaptive algorithms based on primal schemes we mention [5, 4, 29, 38].

Motivated by the discussion above, in this work we provide the *a posteriori* error analysis of the mixed variational formulation introduced in [13]. One of the principal advantages of our Banach space-based approach is that our *a posteriori* error estimator, besides being fully-local and fully-computable, is locally efficient, which improves the results obtained in [20, 17]. In turn, using the associated *a posteriori* error indicator we propose an adaptive algorithm which is of low computational cost, and allows to improve the accuracy, the stability and the robustness of our fully-mixed method when being applied to problems in which the overall approximation quality can be deteriorated by the presence of boundary layers, singularities, or complex geometries.

The rest of this work is organized as follows. In Section 3 we recall from [13] the model problem and its continuous and discrete mixed variational formulations. Next in Section 4 we provide some preliminary results to be employed next to derive and analyze our *a posteriori* error estimator. The kernel of the present work is given by Section 5, where we develop the *a posteriori* error analysis. In Section 5.1 we employ the global continuous inf-sup condition, a suitable Helmholtz decomposition, and the local approximation properties of the Clément and Raviart-Thomas operators, to derive a reliable residual-based *a posteriori* error estimator. Then, in Section 5.2 inverse inequalities, and the localization technique based on element-bubble and edge-bubble functions are utilized to prove the efficiency of the estimator. Finally, numerical results confirming the reliability and efficiency of the *a posteriori* error estimator, and showing the good performance of the associated adaptive algorithm, are presented in Section 6.

## 2 Preliminary notations

Let us denote by  $\Omega \subseteq \mathbb{R}^d$ ,  $d \in \{2, 3\}$ , a given bounded domain with polyhedral boundary  $\Gamma$ . Standard notations will be adopted for Lebesgue spaces  $L^p(\Omega)$ , with  $p \in [1, \infty]$  and Sobolev spaces  $W^{r,p}(\Omega)$  with  $r \geq 0$ , endowed with the norms  $\|\cdot\|_{L^p(\Omega)}$  and  $\|\cdot\|_{W^{r,p}(\Omega)}$ , respectively. Note that  $W^{0,p}(\Omega) = L^p(\Omega)$  and if  $p = 2$ , we write  $H^r(\Omega)$  in place of  $W^{r,2}(\Omega)$ , with the corresponding Lebesgue and Sobolev norms denoted by  $\|\cdot\|_{0,\Omega}$  and  $\|\cdot\|_{r,\Omega}$ , respectively. We also write  $|\cdot|_{r,\Omega}$  for the  $H^r$ -seminorm. In addition,  $H^{1/2}(\Gamma)$  is the spaces of traces of functions of  $H^1(\Omega)$  and  $H^{-1/2}(\Gamma)$  denotes its dual. With  $\langle \cdot, \cdot \rangle$  we denote the corresponding product of duality between  $H^{1/2}(\Gamma)$  and  $H^{-1/2}(\Gamma)$ . By  $\mathbf{S}$  and  $\mathbb{S}$  we will denote the corresponding vectorial and tensorial counterparts of the generic scalar functional space  $S$ . In addition, we will denote by  $\|(u, v)\| := \|(u, v)\|_{U \times V} := \|u\|_U + \|v\|_V$  the norm on the product space  $U \times V$ .

As usual  $\mathbb{I}$  stands for the identity tensor in  $\mathbb{R}^{d \times d}$ , and  $|\cdot|$  denotes the Euclidean norm in  $\mathbb{R}^d$ . Also, for any vector fields  $\mathbf{v} = (v_i)_{i=1,d}$  and  $\mathbf{w} = (w_i)_{i=1,d}$  we set the gradient, divergence, and tensor product operators, as

$$\nabla \mathbf{v} := \left( \frac{\partial v_i}{\partial x_j} \right)_{i,j=1,d}, \quad \operatorname{div} \mathbf{v} := \sum_{j=1}^d \frac{\partial v_j}{\partial x_j}, \quad \text{and} \quad \mathbf{v} \otimes \mathbf{w} := (v_i w_j)_{i,j=1,d}.$$

In addition, for any tensor fields  $\boldsymbol{\tau} = (\tau_{ij})_{i,j=1,d}$  and  $\boldsymbol{\zeta} = (\zeta_{ij})_{i,j=1,d}$ , we let  $\mathbf{div} \boldsymbol{\tau}$  be the divergence operator  $\operatorname{div}$  acting along the rows of  $\boldsymbol{\tau}$ , and define the transpose, the trace, the tensor inner product, and the deviatoric tensor, respectively, as

$$\boldsymbol{\tau}^t := (\tau_{ji})_{i,j=1,d}, \quad \operatorname{tr}(\boldsymbol{\tau}) := \sum_{i=1}^d \tau_{ii}, \quad \boldsymbol{\tau} : \boldsymbol{\zeta} := \sum_{i,j=1}^d \tau_{ij} \zeta_{ij} \quad \text{and} \quad \boldsymbol{\tau}^d := \boldsymbol{\tau} - \frac{1}{d} \operatorname{tr}(\boldsymbol{\tau}) \mathbb{I}.$$

For simplicity, in what follows we denote

$$(v, w)_\Omega := \int_\Omega v w, \quad (\mathbf{v}, \mathbf{w})_\Omega := \int_\Omega \mathbf{v} \cdot \mathbf{w}, \quad (\mathbf{v}, \mathbf{w})_\Gamma := \int_\Gamma \mathbf{v} \cdot \mathbf{w} \quad \text{and} \quad (\boldsymbol{\tau}, \boldsymbol{\zeta})_\Omega := \int_\Omega \boldsymbol{\tau} : \boldsymbol{\zeta}.$$

We also recall the Hilbert space

$$\mathbf{H}(\operatorname{div}; \Omega) := \{\mathbf{z} \in \mathbf{L}^2(\Omega) : \operatorname{div} \mathbf{z} \in L^2(\Omega)\},$$

with norm  $\|\mathbf{z}\|_{\operatorname{div}; \Omega}^2 := \|\mathbf{z}\|_{0,\Omega}^2 + \|\operatorname{div} \mathbf{z}\|_{0,\Omega}^2$ , and introduce the tensor version of  $\mathbf{H}(\operatorname{div}; \Omega)$  given by

$$\mathbb{H}(\mathbf{div}; \Omega) := \{\boldsymbol{\tau} \in \mathbb{L}^2(\Omega) : \mathbf{div} \boldsymbol{\tau} \in \mathbf{L}^2(\Omega)\},$$

whose norm will be denoted by  $\|\cdot\|_{\mathbf{div}; \Omega}$ . Finally, given  $p > \frac{2d}{d+2}$ , in what follows we will also employ the non-standard Banach space  $\mathbb{H}(\mathbf{div}_p, \Omega)$  defined by

$$\mathbb{H}(\mathbf{div}_p; \Omega) := \{\boldsymbol{\tau} \in \mathbb{L}^2(\Omega) : \mathbf{div} \boldsymbol{\tau} \in \mathbf{L}^p(\Omega)\},$$

endowed with the norm

$$\|\boldsymbol{\tau}\|_{\mathbf{div}_p; \Omega} := \left( \|\boldsymbol{\tau}\|_{0,\Omega}^2 + \|\mathbf{div} \boldsymbol{\tau}\|_{\mathbf{L}^p(\Omega)}^2 \right)^{1/2}.$$

## 3 The model problem and its momentum and thermal energy conservative formulation

In this section we recall from [13] the steady-state natural convection model, its variational formulation, the associated Galerkin scheme, and the main results concerning the corresponding solvability analysis.

### 3.1 The steady-state natural convection model

The stationary Boussinesq problem is a system of equations where the incompressible Navier–Stokes equation:

$$\begin{aligned} -\nu \Delta \mathbf{u} + (\nabla \mathbf{u})\mathbf{u} + \nabla p - \theta \mathbf{g} &= \mathbf{0} \quad \text{in } \Omega, \quad \operatorname{div} \mathbf{u} = 0 \quad \text{in } \Omega, \\ \mathbf{u} &= \mathbf{0} \quad \text{on } \Gamma, \quad (p, 1)_\Omega = 0, \end{aligned} \quad (3.1)$$

is coupled with the convection-diffusion equation:

$$-\kappa \Delta \theta + \mathbf{u} \cdot \nabla \theta = 0 \quad \text{in } \Omega, \quad \theta = \theta_D \quad \text{on } \Gamma_D, \quad \kappa \nabla \theta \cdot \mathbf{n} = 0 \quad \text{on } \Gamma_N. \quad (3.2)$$

Here  $\Omega$  is a bounded domain in  $\mathbb{R}^d$ ,  $d \in \{2, 3\}$ , with polyhedral boundary  $\Gamma$ . The unknowns are the velocity  $\mathbf{u}$ , the pressure  $p$  and the temperature  $\theta$  of the fluid occupying the region  $\Omega$ , and the given data are the fluid viscosity  $\nu > 0$ , the thermal conductivity  $\kappa > 0$ , the external force per unit mass  $\mathbf{g} \in \mathbf{L}^2(\Omega)$ , and the boundary temperature  $\theta_D \in H^{1/2}(\Gamma_D)$ .

Now, in order to derive our approach (see [13, Section 2] for details), we begin by introducing the tensor and vector variables

$$\boldsymbol{\sigma} := \nu \nabla \mathbf{u} - (\mathbf{u} \otimes \mathbf{u}) - p \mathbb{I} \quad \text{and} \quad \boldsymbol{\rho} := \kappa \nabla \theta - \theta \mathbf{u} \quad \text{in } \Omega,$$

and utilize the incompressibility condition  $\operatorname{div} \mathbf{u} = \operatorname{tr}(\nabla \mathbf{u}) = 0$  in  $\Omega$  to rewrite the systems (3.1) and (3.2), respectively as the following equivalent first-order set of equations (see [10] and [20] for details):

$$\begin{aligned} \frac{1}{\nu} \boldsymbol{\sigma}^d + \frac{1}{\nu} (\mathbf{u} \otimes \mathbf{u})^d &= \nabla \mathbf{u} \quad \text{in } \Omega, \quad \operatorname{div} \boldsymbol{\sigma} + \theta \mathbf{g} = \mathbf{0} \quad \text{in } \Omega, \\ p &= -\frac{1}{d} \operatorname{tr}(\boldsymbol{\sigma} + \mathbf{u} \otimes \mathbf{u}) \quad \text{in } \Omega, \quad \mathbf{u} = \mathbf{0} \quad \text{on } \Gamma, \quad (\operatorname{tr}(\boldsymbol{\sigma} + \mathbf{u} \otimes \mathbf{u}), 1)_\Omega = 0, \end{aligned} \quad (3.3)$$

and

$$\begin{aligned} \kappa^{-1} \boldsymbol{\rho} + \kappa^{-1} \theta \mathbf{u} &= \nabla \theta \quad \text{in } \Omega, \quad \operatorname{div} \boldsymbol{\rho} = 0 \quad \text{in } \Omega, \\ \theta &= \theta_D \quad \text{on } \Gamma_D, \quad \boldsymbol{\rho} \cdot \mathbf{n} = 0 \quad \text{on } \Gamma_N. \end{aligned} \quad (3.4)$$

Notice that the third equation in (3.3) has allowed us to eliminate the pressure  $p$  from the system and provides a formula for its approximation through a post-processing procedure, whereas the last equation takes care of the requirement that  $(p, 1)_\Omega = 0$ .

### 3.2 The continuous weak formulation and its well posedness

In this section, we recall from [13, Section 2] the weak formulation of the problem given by (3.3)–(3.4). To that end, we define the spaces

$$\begin{aligned} \mathbb{X} &:= \mathbb{H}(\operatorname{div}_{4/3}; \Omega), \quad \mathbf{M} := \mathbf{L}^4(\Omega), \\ \mathbf{H} &:= \left\{ \boldsymbol{\eta} \in \mathbf{H}(\operatorname{div}_{4/3}; \Omega) : \boldsymbol{\eta} \cdot \mathbf{n} = 0 \quad \text{on } \Gamma_N \right\}, \quad \mathbf{Q} := \mathbf{L}^4(\Omega), \end{aligned}$$

and

$$\mathbb{X}_0 := \left\{ \boldsymbol{\tau} \in \mathbb{H}(\operatorname{div}_{4/3}; \Omega) : (\operatorname{tr}(\boldsymbol{\tau}), 1)_\Omega = 0 \right\},$$

and observe that the following decomposition holds:

$$\mathbb{X} = \mathbb{X}_0 \oplus \mathbf{P}_0(\Omega) \mathbf{I},$$

where  $P_0(\Omega)$  is the space of constant polynomials on  $\Omega$ .

The derivation of the weak formulation proposed in [13] for the problem given by (3.3)–(3.4) relies on the previous orthogonal decomposition. In fact, it can be proved that the uniqueness condition given by the last equation in (3.3) allows us to only look for the  $\mathbb{X}_0$ –component of the tensor  $\boldsymbol{\sigma}$  (cf. [10, Lemma 3.1]). Therefore, the variational formulation of (3.3)–(3.4) reads: Find  $(\boldsymbol{\sigma}, \mathbf{u}, \boldsymbol{\rho}, \theta) \in \mathbb{X}_0 \times \mathbf{M} \times \mathbf{H} \times \mathbf{Q}$ , such that:

$$\begin{aligned} a_F(\boldsymbol{\sigma}, \boldsymbol{\tau}) + b_F(\boldsymbol{\tau}, \mathbf{u}) + c_F(\mathbf{u}; \mathbf{u}, \boldsymbol{\tau}) &= 0 & \forall \boldsymbol{\tau} \in \mathbb{X}_0, \\ b_F(\boldsymbol{\sigma}, \mathbf{v}) + d_F(\theta, \mathbf{v}) &= 0 & \forall \mathbf{v} \in \mathbf{M}, \\ a_T(\boldsymbol{\rho}, \boldsymbol{\eta}) + b_T(\boldsymbol{\eta}, \theta) + c_T(\mathbf{u}; \theta, \boldsymbol{\eta}) &= F_T(\boldsymbol{\eta}) & \forall \boldsymbol{\eta} \in \mathbf{H}, \\ b_T(\boldsymbol{\rho}, \psi) &= 0 & \forall \psi \in \mathbf{Q}, \end{aligned} \quad (3.5)$$

where, the bounded forms  $a_F : \mathbb{X} \times \mathbb{X} \rightarrow \mathbb{R}$ ,  $b_F : \mathbb{X} \times \mathbf{M} \rightarrow \mathbb{R}$ ,  $c_F : \mathbf{M} \times \mathbf{M} \times \mathbb{X} \rightarrow \mathbb{R}$ ,  $d_F : \mathbf{Q} \times \mathbf{M} \rightarrow \mathbb{R}$ ,  $a_T : \mathbf{H} \times \mathbf{H} \rightarrow \mathbb{R}$ ,  $b_T : \mathbf{H} \times \mathbf{Q} \rightarrow \mathbb{R}$ , and  $c_T : \mathbf{M} \times \mathbf{Q} \times \mathbf{H} \rightarrow \mathbb{R}$  are defined as:

$$\begin{aligned} a_F(\boldsymbol{\sigma}, \boldsymbol{\tau}) &:= \frac{1}{\nu} (\boldsymbol{\sigma}^d, \boldsymbol{\tau}^d)_\Omega, & b_F(\boldsymbol{\tau}, \mathbf{v}) &:= (\mathbf{v}, \operatorname{div} \boldsymbol{\tau})_\Omega, \\ c_F(\mathbf{w}; \mathbf{u}, \boldsymbol{\tau}) &:= \frac{1}{\nu} ((\mathbf{w} \otimes \mathbf{u})^d, \boldsymbol{\tau})_\Omega, & d_F(\theta, \mathbf{v}) &:= (\theta \mathbf{g}, \mathbf{v})_\Omega, \\ a_T(\boldsymbol{\rho}, \boldsymbol{\eta}) &:= \kappa^{-1} (\boldsymbol{\rho}, \boldsymbol{\eta})_\Omega, & b_T(\boldsymbol{\eta}, \psi) &:= (\psi, \operatorname{div} \boldsymbol{\eta})_\Omega, \\ c_T(\mathbf{w}; \theta, \boldsymbol{\eta}) &:= \kappa^{-1} (\theta \mathbf{w}, \boldsymbol{\eta})_\Omega, \end{aligned} \quad (3.6)$$

and the functional  $F_T \in \mathbf{H}'$ :

$$F_T(\boldsymbol{\eta}) := \langle \boldsymbol{\eta} \cdot \mathbf{n}, \theta_D \rangle_{\Gamma_D}. \quad (3.7)$$

This problem is analyzed throughout [13, Section 3], and the well-posedness comes as a result of a fixed-point strategy. In particular, we recall from [13] the following inf-sup conditions: Given  $\mathbf{u} \in \mathbf{M}$  such that  $\|\mathbf{u}\|_{\mathbf{M}} \leq \frac{\lambda}{2}$ , with  $\lambda := \min\{\nu \gamma_F, \kappa \gamma_T\}$ , there holds

$$\sup_{\substack{(\boldsymbol{\tau}, \mathbf{v}) \in \mathbb{X}_0 \times \mathbf{M} \\ (\boldsymbol{\tau}, \mathbf{v}) \neq \mathbf{0}}} \frac{|a_F(\boldsymbol{\zeta}, \boldsymbol{\tau}) + b_F(\boldsymbol{\tau}, \mathbf{z}) + b_F(\boldsymbol{\zeta}, \mathbf{v}) + c_F(\mathbf{u}; \mathbf{z}, \boldsymbol{\tau})|}{\|(\boldsymbol{\tau}, \mathbf{v})\|} \geq \frac{\gamma_F}{2} \|(\boldsymbol{\zeta}, \mathbf{z})\| \quad \forall (\boldsymbol{\zeta}, \mathbf{z}) \in \mathbb{X}_0 \times \mathbf{M}, \quad (3.8)$$

and

$$\sup_{\substack{(\boldsymbol{\eta}, \psi) \in \mathbf{H} \times \mathbf{Q} \\ (\boldsymbol{\eta}, \psi) \neq \mathbf{0}}} \frac{|a_T(\boldsymbol{\varsigma}, \boldsymbol{\eta}) + b_T(\boldsymbol{\eta}, \varphi) + b_T(\boldsymbol{\varsigma}, \psi) + c_T(\mathbf{u}; \varphi, \boldsymbol{\eta})|}{\|(\boldsymbol{\eta}, \psi)\|} \geq \frac{\gamma_T}{2} \|(\boldsymbol{\varsigma}, \varphi)\| \quad \forall (\boldsymbol{\varsigma}, \varphi) \in \mathbf{H} \times \mathbf{Q}, \quad (3.9)$$

with

$$\gamma_F := C \frac{\min\{1, \nu \beta_F\}}{\nu \beta_F + 1} \quad \text{and} \quad \gamma_T := \frac{\kappa \beta_T^2}{\kappa^2 \beta_T^2 + 4 \kappa \beta_T + 2}, \quad (3.10)$$

where  $C$ ,  $\beta_F$  and  $\beta_T$  are positive constants independent of the physical parameters. In particular,  $\beta_F$  and  $\beta_T$  are the constants related with the inf-sup conditions of the bilinear forms  $b_F$  and  $b_T$ , respectively (cf. [10, Lemma 3.4] and [13, Lemma 3.1]).

In turn, the following result taken from [13] establishes the well-posedness of (3.5).

**Theorem 3.1** Let define  $\lambda := \min \{ \nu \gamma_F, \kappa \gamma_T \}$  and assume that

$$\frac{16 C_F}{\lambda \gamma_F \gamma_T} \|\mathbf{g}\|_{0,\Omega} \|\theta_D\|_{1/2,\Gamma_D} < 1,$$

where  $C_F$  is the bounding constant of  $F_T$ , and  $\gamma_F$  and  $\gamma_T$  are the constants defined in (3.10). Then, the coupled problem (3.5) has a unique solution  $(\boldsymbol{\sigma}, \mathbf{u}, \boldsymbol{\rho}, \theta) \in \mathbb{X}_0 \times \mathbf{M} \times \mathbf{H} \times \mathbf{Q}$ . Moreover, there hold

$$\|(\boldsymbol{\sigma}, \mathbf{u})\| \leq \frac{4 C_F}{\gamma_F \gamma_T} \|\mathbf{g}\|_{0,\Omega} \|\theta_D\|_{1/2,\Gamma_D} \quad \text{and} \quad \|(\boldsymbol{\rho}, \theta)\| \leq \frac{2 C_F}{\gamma_T} \|\theta_D\|_{1/2,\Gamma_D}. \quad (3.11)$$

*Proof.* See [13, Theorem 3.2] for details.  $\square$

We now provide the converse of the derivation of (3.5).

**Theorem 3.2** Let  $(\boldsymbol{\sigma}, \mathbf{u}, \boldsymbol{\rho}, \theta) \in \mathbb{X}_0 \times \mathbf{M} \times \mathbf{H} \times \mathbf{Q}$  be the unique solution of the variational formulation (3.5). Then,  $\frac{1}{\nu} \boldsymbol{\sigma}^d + \frac{1}{\nu} (\mathbf{u} \otimes \mathbf{u})^d = \nabla \mathbf{u}$  in  $\Omega$ ,  $\mathbf{u} \in \mathbf{H}^1(\Omega)$ ,  $\operatorname{div} \boldsymbol{\sigma} + \theta \mathbf{g} = \mathbf{0}$  in  $\Omega$ ,  $\mathbf{u} = \mathbf{0}$  on  $\Gamma$ ,  $\kappa^{-1} \boldsymbol{\rho} + \kappa^{-1} \theta \mathbf{u} = \nabla \theta$  in  $\Omega$ ,  $\theta \in H^1(\Omega)$ ,  $\operatorname{div} \boldsymbol{\rho} = 0$  in  $\Omega$ ,  $\theta = \theta_D$  on  $\Gamma_D$  and  $\boldsymbol{\rho} \cdot \mathbf{n} = 0$  on  $\Gamma_N$ .

*Proof.* First, it is clear that the identities  $\operatorname{div} \boldsymbol{\sigma} + \theta \mathbf{g} = \mathbf{0}$  in  $\Omega$  and  $\operatorname{div} \boldsymbol{\rho} = 0$  in  $\Omega$  follow from the second and fourth equations of (3.5), respectively. The derivation of the rest of the identities follows from the first and third equations of (3.5), considering suitable test functions and integrating by parts backwardly. We omit further details.  $\square$

### 3.3 The discrete coupled system and its well-posedness

Let us begin by considering  $\{\mathcal{T}_h\}_{h>0}$  a family of regular triangulations of  $\bar{\Omega}$  made by triangles  $T$  (when  $d = 2$ ) or tetrahedra (when  $d = 3$ ) of diameter  $h_T$  and define the meshsize  $h := \max \{h_T : T \in \mathcal{T}_h\}$ . Given an integer  $l \geq 0$  and a subset  $S$  of  $\mathbb{R}^d$ , we denote by  $P_l(S)$  the space of polynomials of total degree at most  $l$  defined on  $S$ . Hence, for each integer  $k \geq 0$  and for each  $T \in \mathcal{T}_h$ , we define the local Raviart–Thomas space of order  $k$  as (see, for instance [8]):

$$\mathbf{RT}_k(T) := [P_k(T)]^d \oplus \tilde{P}_k(T) \mathbf{x},$$

where  $\mathbf{x} := (x_1, \dots, x_d)^t$  is a generic vector of  $\mathbb{R}^d$  and  $\tilde{P}_k(T)$  is the space of polynomials of total degree equal to  $k$  defined on  $T$ . In this way, we define the finite element subspaces:

$$\begin{aligned} \mathbb{X}_h &:= \left\{ \boldsymbol{\tau}_h \in \mathbb{X} : \quad \mathbf{c}^t \boldsymbol{\tau}_h|_T \in \mathbf{RT}_k(T) \quad \forall \mathbf{c} \in \mathbb{R}^d \quad \forall T \in \mathcal{T}_h \right\}, \\ \mathbf{M}_h &:= \left\{ \mathbf{v}_h \in \mathbf{M} : \quad \mathbf{v}_h|_T \in [P_k(T)]^d \quad \forall T \in \mathcal{T}_h \right\}, \\ \mathbf{H}_h &:= \left\{ \boldsymbol{\eta}_h \in \mathbf{H} : \quad \boldsymbol{\eta}_h|_T \in \mathbf{RT}_k(T) \quad \forall T \in \mathcal{T}_h \right\}, \\ \mathbf{Q}_h &:= \left\{ \phi_h \in \mathbf{Q} : \quad \phi_h|_T \in P_k(T) \quad \forall T \in \mathcal{T}_h \right\}. \end{aligned} \quad (3.12)$$

Then defining the subspace  $\mathbb{X}_{h,0} := \mathbb{X}_h \cap \mathbb{X}_0$ , the Galerkin scheme associated to problem (3.5) reads: Find  $(\boldsymbol{\sigma}_h, \mathbf{u}_h, \boldsymbol{\rho}_h, \theta_h) \in \mathbb{X}_{h,0} \times \mathbf{M}_h \times \mathbf{H}_h \times \mathbf{Q}_h$  such that:

$$\begin{aligned} a_F(\boldsymbol{\sigma}_h, \boldsymbol{\tau}_h) + b_F(\boldsymbol{\tau}_h, \mathbf{u}_h) + c_F(\mathbf{u}_h; \mathbf{u}_h, \boldsymbol{\tau}_h) &= 0 & \forall \boldsymbol{\tau}_h \in \mathbb{X}_{h,0} \\ b_F(\boldsymbol{\sigma}_h, \mathbf{v}_h) + d_F(\theta_h, \mathbf{v}_h) &= 0 & \forall \mathbf{v}_h \in \mathbf{M}_h \\ a_T(\boldsymbol{\rho}_h, \boldsymbol{\eta}_h) + b_T(\boldsymbol{\eta}_h, \theta_h) + c_T(\mathbf{u}_h; \theta_h, \boldsymbol{\eta}_h) &= F_T(\boldsymbol{\eta}_h) & \forall \boldsymbol{\eta}_h \in \mathbf{H}_h \\ b_T(\boldsymbol{\rho}_h, \psi_h) &= 0 & \forall \psi_h \in \mathbf{Q}_h \end{aligned} \quad (3.13)$$



where the forms  $a_F, b_F, c_F, d_F, a_T, b_T, c_T$  and the functional  $F_T$  are defined in (3.6) and (3.7), respectively.

The following results, taken from [13, Theorem 4.1 and Theorem 5.2], provides the well-posedness of (3.13) and the corresponding theoretical rate of convergence.

**Theorem 3.3** *Assume that there exists a convex domain  $B$  such that  $\Omega \subseteq B$  and  $\Gamma_N \subseteq \partial B$ . Let define  $\widehat{\lambda} := \min \{ \nu \widehat{\gamma}_F, \kappa \widehat{\gamma}_T \}$  and assume that*

$$\frac{16 C_F}{\widehat{\lambda} \widehat{\gamma}_F \widehat{\gamma}_T} \|\mathbf{g}\|_{0,\Omega} \|\theta_D\|_{1/2,\Gamma_D} < 1,$$

where  $C_F$  is the bounding constant of  $F_T$ , and  $\widehat{\gamma}_F$  and  $\widehat{\gamma}_T$  are the discrete version of  $\gamma_F$  and  $\gamma_T$  respectively (cf. (3.10)), given by

$$\widehat{\gamma}_F := C \frac{\min\{1, \nu \widehat{\beta}_F\}}{\nu \widehat{\beta}_F + 1} \quad \text{and} \quad \widehat{\gamma}_T := \frac{\kappa \widehat{\beta}_T^2}{\kappa^2 \widehat{\beta}_T^2 + 4 \kappa \widehat{\beta}_T + 2}, \quad (3.14)$$

where  $C$  is a positive constant independent of the physical parameters, and  $\widehat{\beta}_F$  and  $\widehat{\beta}_T$  are the constants related with the discrete inf-sup conditions of the bilinear forms  $b_F$  and  $b_T$ , respectively. Then, the coupled problem (3.13) has a unique solution  $(\boldsymbol{\sigma}_h, \mathbf{u}_h, \boldsymbol{\rho}_h, \theta_h) \in \mathbb{X}_{h,0} \times \mathbf{M}_h \times \mathbf{H}_h \times \mathbf{Q}_h$ . Moreover, there hold

$$\|(\boldsymbol{\sigma}_h, \mathbf{u}_h)\| \leq \frac{4 C_F}{\widehat{\gamma}_F \widehat{\gamma}_T} \|\mathbf{g}\|_{0,\Omega} \|\theta_D\|_{1/2,\Gamma_D} \quad \text{and} \quad \|(\boldsymbol{\rho}_h, \theta_h)\| \leq \frac{2 C_F}{\widehat{\gamma}_T} \|\theta_D\|_{1/2,\Gamma_D}. \quad (3.15)$$

**Theorem 3.4** *Assume that there exists a convex domain  $B$  such that  $\Omega \subseteq B$  and  $\Gamma_N \subseteq \partial B$ . Let define  $\widetilde{\lambda} := \min \{ \nu \gamma_F, \kappa \gamma_T \}$  and assume further that*

$$\frac{16 C_F}{\widetilde{\lambda} \gamma_F \gamma_T} \|\mathbf{g}\|_{0,\Omega} \|\theta_D\|_{1/2,\Gamma_D} \leq \frac{1}{2},$$

where  $C_F$  is the bounding constant of  $F_T$ , and  $\gamma_F, \gamma_T$  and  $\widehat{\gamma}_F, \widehat{\gamma}_T$  given in (3.10) and (3.14), respectively. Let  $(\boldsymbol{\sigma}, \mathbf{u}, \boldsymbol{\rho}, \theta) \in \mathbb{X}_0 \times \mathbf{M} \times \mathbf{H} \times \mathbf{Q}$  and  $(\boldsymbol{\sigma}_h, \mathbf{u}_h, \boldsymbol{\rho}_h, \theta_h) \in \mathbb{X}_{h,0} \times \mathbf{M}_h \times \mathbf{H}_h \times \mathbf{Q}_h$  be the unique solutions of the continuous and discrete problems (3.5) and (3.13), respectively. Assume further that  $\boldsymbol{\sigma} \in \mathbb{H}^{l+1}(\Omega)$ ,  $\text{div} \boldsymbol{\sigma} \in \mathbf{W}^{l+1,4/3}(\Omega)$ ,  $\mathbf{u} \in \mathbf{W}^{l+1,4}(\Omega)$ ,  $\boldsymbol{\rho} \in \mathbf{H}^{l+1}(\Omega)$ ,  $\text{div} \boldsymbol{\rho} \in \mathbf{W}^{l+1,4/3}(\Omega)$  and  $\theta \in \mathbf{W}^{l+1,4}(\Omega)$ , for  $0 \leq l \leq k$ . Then there exists  $C_{\text{rate}} > 0$ , independent of  $h$ , but depending on the domain,  $\nu, \kappa, \|\mathbf{g}\|_{0,\Omega}$ , and the datum  $\theta_D$ , such that

$$\begin{aligned} \|(\boldsymbol{\sigma}, \mathbf{u}) - (\boldsymbol{\sigma}_h, \mathbf{u}_h)\| + \|(\boldsymbol{\rho}, \theta) - (\boldsymbol{\rho}_h, \theta_h)\| &\leq C_{\text{rate}} h^{l+1} \left\{ \|\boldsymbol{\sigma}\|_{l+1,\Omega} + \|\text{div} \boldsymbol{\sigma}\|_{\mathbf{W}^{l+1,4/3}(\Omega)} \right. \\ &\quad \left. + \|\mathbf{u}\|_{\mathbf{W}^{l+1,4}(\Omega)} + \|\boldsymbol{\rho}\|_{l+1,\Omega} + \|\text{div} \boldsymbol{\rho}\|_{\mathbf{W}^{l+1,4/3}(\Omega)} + \|\theta\|_{\mathbf{W}^{l+1,4}(\Omega)} \right\}. \end{aligned}$$

## 4 Preliminaries for the a posteriori error analysis

We start by introducing a few useful notations for describing local information on elements and edges or faces depending on whether  $d = 2$  or  $d = 3$ , respectively. Let  $\mathcal{E}_h$  be the set of edges or faces of  $\mathcal{T}_h$ , whose corresponding diameters are denoted by  $h_e$ , and define

$$\mathcal{E}_h(\Omega) := \{ e \in \mathcal{E}_h : e \subseteq \Omega \} \quad \text{and} \quad \mathcal{E}_h(\Gamma) := \{ e \in \mathcal{E}_h : e \subseteq \Gamma \}.$$

For each  $T \in \mathcal{T}_h$ , we let  $\mathcal{E}_{h,T}$  be the set of edges or faces of  $T$ , and denote

$$\mathcal{E}_{h,T}(\Omega) = \{ e \subseteq \partial T : e \in \mathcal{E}_h(\Omega) \} \quad \text{and} \quad \mathcal{E}_{h,T}(\Gamma) = \{ e \subseteq \partial T : e \in \mathcal{E}_h(\Gamma) \}.$$

We also define the unit normal vector  $\mathbf{n}_e$  on each edge or face by

$$\mathbf{n}_e := (n_1, \dots, n_d)^t \quad \forall e \in \mathcal{E}_h.$$

Hence, when  $d = 2$  we can define the tangential vector  $\mathbf{s}_e$  by

$$\mathbf{s}_e := (-n_2, n_1)^t \quad \forall e \in \mathcal{E}_h.$$

However, when no confusion arises, we will simply write  $\mathbf{n}$  and  $\mathbf{s}$  instead of  $\mathbf{n}_e$  and  $\mathbf{s}_e$ , respectively.

The usual jump operator  $[\![\cdot]\!]$  across internal edges or faces are defined for piecewise continuous matrix, vector, or scalar-valued functions  $\boldsymbol{\zeta}$ , by

$$[\![\boldsymbol{\zeta}]\!] = (\boldsymbol{\zeta}|_{T_+})|_e - (\boldsymbol{\zeta}|_{T_-})|_e \quad \text{with } e = \partial T_+ \cap \partial T_-,$$

where  $T_+$  and  $T_-$  are the elements of  $\mathcal{T}_h$  having  $e$  as a common edge or face. Finally, for sufficiently smooth scalar  $\psi$ , vector  $\mathbf{v} := (v_1, \dots, v_d)^t$ , and tensor fields  $\boldsymbol{\tau} := (\tau_{ij})_{1 \leq i, j \leq d}$ , we let

$$\begin{aligned} \text{curl}(\psi) &:= \left( -\frac{\partial \psi}{\partial x_2}, \frac{\partial \psi}{\partial x_1} \right)^t, \quad \text{for } d = 2, \\ \underline{\text{curl}}(\mathbf{v}) &= \begin{cases} \frac{\partial \mathbf{v}_2}{\partial x_1} - \frac{\partial \mathbf{v}_1}{\partial x_2} & , \text{ for } d = 2, \\ \nabla \times \mathbf{v} & , \text{ for } d = 3, \end{cases} \quad \underline{\text{curl}}(\boldsymbol{\tau}) = \begin{cases} \begin{pmatrix} \underline{\text{curl}}(\boldsymbol{\tau}_1) \\ \underline{\text{curl}}(\boldsymbol{\tau}_2) \end{pmatrix} & , \text{ for } d = 2, \\ \begin{pmatrix} \underline{\text{curl}}(\boldsymbol{\tau}_1) \\ \underline{\text{curl}}(\boldsymbol{\tau}_2) \\ \underline{\text{curl}}(\boldsymbol{\tau}_3) \end{pmatrix} & , \text{ for } d = 3, \end{cases} \\ \boldsymbol{\gamma}_*(\mathbf{v}) &= \begin{cases} \mathbf{v} \cdot \mathbf{s} & , \text{ for } d = 2, \\ \mathbf{v} \times \mathbf{n} & , \text{ for } d = 3, \end{cases} \quad \text{and} \quad \boldsymbol{\gamma}_*(\boldsymbol{\tau}) = \begin{cases} \boldsymbol{\tau} \mathbf{s} & , \text{ for } d = 2, \\ \begin{pmatrix} \boldsymbol{\tau}_1 \times \mathbf{n} \\ \boldsymbol{\tau}_2 \times \mathbf{n} \\ \boldsymbol{\tau}_3 \times \mathbf{n} \end{pmatrix} & , \text{ for } d = 3, \end{cases} \end{aligned}$$

where  $\boldsymbol{\tau}_i$  is the  $i$ -th row of  $\boldsymbol{\tau}$  and the derivatives involved are taken in the distributional sense.

Let us now recall the main properties of the Raviart–Thomas interpolator (see e.g. [22]) and the Cl  ment operator (see e.g. [14]) onto the space of continuous piecewise linear functions. Given  $p > 1$ , let us define the space

$$\mathbf{Z}_p := \{ \boldsymbol{\tau} \in \mathbf{H}(\text{div}_p; \Omega) : \boldsymbol{\tau}|_T \in \mathbf{W}^{1,p}(T), \quad \forall T \in \mathcal{T}_h \},$$

and let

$$\Pi_h^k : \mathbf{Z}_p \rightarrow \mathbf{X}_h := \{ \boldsymbol{\tau} \in \mathbf{H}(\text{div}; \Omega) : \boldsymbol{\tau}|_T \in \mathbf{RT}_k(T), \quad \forall T \in \mathcal{T}_h \},$$

be the Raviart–Thomas interpolation operator, which is well defined in  $\mathbf{Z}_p$  (see e.g. [22, Section 1.2.7]) and is characterized by the identities

$$(\Pi_h^k(\boldsymbol{\tau}) \cdot \mathbf{n}, \xi)_e = (\boldsymbol{\tau} \cdot \mathbf{n}, \xi)_e \quad \forall \xi \in P_k(e), \quad \forall \text{ edge or face } e \text{ of } \mathcal{T}_h, \quad (4.1)$$

and

$$(\Pi_h^k(\boldsymbol{\tau}), \psi)_T = (\boldsymbol{\tau}, \psi)_T \quad \forall \psi \in [P_{k-1}(T)]^d, \quad \forall T \in \mathcal{T}_h \text{ (if } k \geq 1 \text{)}.$$

Notice that, since  $\Pi_h^k(\boldsymbol{\tau}) \cdot \mathbf{n}_e \in P_k(e)$ , from (4.1) we have that

$$\Pi_h^k(\boldsymbol{\tau}) \cdot \mathbf{n}_e = \mathcal{P}_e^k(\boldsymbol{\tau} \cdot \mathbf{n}_e),$$

where, for  $1 \leq r \leq \infty$ ,  $\mathcal{P}_e^k : L^r(e) \rightarrow P_k(e)$  is the operator satisfying

$$\int_e (\mathcal{P}_e^k(v) - v) z_h = 0 \quad \forall z_h \in P_k(e),$$

Notice that for  $r = 2$ ,  $\mathcal{P}_e^k$  coincides with the usual orthogonal projection. In addition, it is well known (see, e.g., [22, Lemma 1.41]) that the following identity holds

$$\operatorname{div} (\Pi_h^k(\tau)) = \mathcal{P}_h^k(\operatorname{div} \tau) \quad \forall \tau \in \mathbf{Z}_p,$$

where, given  $1 \leq r \leq \infty$ ,  $\mathcal{P}_h^k : L^r(\Omega) \rightarrow M_h := \{v \in L^2(\Omega) : v|_T \in P_k(T) \quad \forall T \in \mathcal{T}_h\}$  is the operator satisfying

$$\int_\Omega (\mathcal{P}_h^k(v) - v) z_h = 0 \quad \forall z_h \in M_h.$$

The following lemma establishes the local approximation properties of  $\Pi_h^k$ .

**Lemma 4.1** *Let  $p > 1$ . Then, there exists  $c_1 > 0$ , independent of  $h$ , such that for each  $\tau \in \mathbf{W}^{l+1,p}(T)$  with  $0 \leq l \leq k$ , and for each  $0 \leq m \leq l+1$ , there holds*

$$|\tau - \Pi_h^k(\tau)|_{\mathbf{W}^{m,p}(T)} \leq c_1 \frac{h_T^{l+2}}{\rho_T^{m+1}} |\tau|_{\mathbf{W}^{l+1,p}(T)},$$

where  $\rho_T$  is the diameter of the largest sphere contained in  $T$ . Moreover, there exists  $c_2 > 0$ , independent of  $h$ , such that for each  $\tau \in \mathbf{W}^{1,p}(T)$ , with  $\operatorname{div} \tau \in W^{l+1,p}(T)$  and  $0 \leq l \leq k$ , and for each  $0 \leq m \leq l+1$ , there holds

$$|\operatorname{div} \tau - \operatorname{div} (\Pi_h^k(\tau))|_{W^{m,p}(T)} \leq c_2 \frac{h_T^{l+1}}{\rho_T^m} |\operatorname{div} \tau|_{W^{l+1,p}(T)}.$$

*Proof.* See [10, Lemma 4.1] for details.  $\square$

The following lemma extends the estimate of the normal component of the interpolation error, originally given for Hilbert spaces (see, for instance [26, Lemma 3.18]), to the  $L^p$  case.

**Lemma 4.2** *Let  $p > 1$ ,  $T \in \mathcal{T}_h$  and  $e \in \mathcal{E}_{h,T}$ . Then, there exists  $C > 0$ , independent of  $h$ , such that*

$$\|\tau \cdot \mathbf{n} - \Pi_h^k(\tau) \cdot \mathbf{n}\|_{L^p(e)} \leq C h_e^{1-1/p} |\tau|_{\mathbf{W}^{1,p}(T)} \quad \forall \tau \in \mathbf{W}^{1,p}(T). \quad (4.2)$$

*Proof.* See [9, Lemma 4.2] for details.  $\square$

Now, we consider the space  $H_h^1 = \{v_h \in C(\bar{\Omega}) : v_h|_T \in P_1(T) \quad \forall T \in \mathcal{T}_h\}$  and denote by  $I_h : H^1(\Omega) \rightarrow H_h^1$  the Clément interpolation operator. The local approximation properties of this operator are established in the following lemma (see [14]):

**Lemma 4.3** *There exist constants  $c_1, c_2 > 0$ , independent of  $h$ , such that for all  $v \in H^1(\Omega)$  there holds*

$$\|v - I_h v\|_{0,T} \leq c_1 h_T |v|_{1,\Delta(T)} \quad \forall T \in \mathcal{T}_h,$$

and

$$\|v - I_h v\|_{0,e} \leq c_2 h_e^{1/2} \|v\|_{1,\Delta(e)} \quad \forall e \in \mathcal{E}_h,$$

where  $\Delta(T)$  and  $\Delta(e)$  are the unions of all elements intersecting  $T$  and  $e$ , respectively.

In what follows, we denote by  $\mathbf{\Pi}_h^k : \mathbb{Z}_p \rightarrow \mathbb{X}_h$  the tensor version of  $\Pi_h^k$ , which is defined row-wise by  $\Pi_h^k$  and by  $\mathbf{I}_h : \mathbf{H}^1(\Omega) \rightarrow \mathbf{H}_h^1$  the corresponding vectorial version of  $I_h$  which is defined componentwise by  $I_h$ .

We end this section by establishing a suitable Helmholtz decomposition for

$$\mathbf{H} := \left\{ \boldsymbol{\eta} \in \mathbf{H}(\operatorname{div}_{4/3}; \Omega) : \quad \boldsymbol{\eta} \cdot \mathbf{n} = 0 \quad \text{on} \quad \Gamma_N \right\}.$$

**Lemma 4.4** *Assume that there exists a convex domain  $B$  such that  $\Omega \subseteq B$  and  $\Gamma_N \subseteq \partial B$ , and let  $p > 1$ . Then, for each  $\boldsymbol{\eta} \in \mathbf{H}$  there exist*

$$a) \quad \boldsymbol{\xi} \in \mathbf{W}^{1,p}(\Omega) \text{ and } w \in H_{\Gamma_N}^1(\Omega) \text{ such that } \boldsymbol{\eta} = \boldsymbol{\xi} + \operatorname{curl} w \text{ when } d = 2,$$

$$b) \quad \boldsymbol{\xi} \in \mathbf{W}^{1,p}(\Omega) \text{ and } \mathbf{w} \in \mathbf{H}_{\Gamma_N}^1(\Omega) \text{ such that } \boldsymbol{\eta} = \boldsymbol{\xi} + \underline{\operatorname{curl}} \mathbf{w} \text{ when } d = 3,$$

where  $H_{\Gamma_N}^1(\Omega) := \left\{ w \in H^1(\Omega) : \quad w = 0 \quad \text{on} \quad \Gamma_N \right\}$ . In addition, we have that

$$\|\boldsymbol{\xi}\|_{\mathbf{W}^{1,p}(\Omega)} + \|w\|_{1,\Omega} \leq C_{Hel} \|\boldsymbol{\eta}\|_{\operatorname{div}_p;\Omega} \quad \text{and} \quad \|\boldsymbol{\xi}\|_{\mathbf{W}^{1,p}(\Omega)} + \|\mathbf{w}\|_{1,\Omega} \leq C_{Hel} \|\boldsymbol{\eta}\|_{\operatorname{div}_p;\Omega}, \quad (4.3)$$

for  $d = 2$  and  $d = 3$ , respectively, where  $C_{Hel}$  is a positive constant independent of all the foregoing variables.

*Proof.* In what follows we prove the result for the two-dimensional case. The three-dimensional case can be treated similarly by extending [25, Theorem 3.1] to the  $L^p$  case.

We proceed as in the proof of [7, Lemma 3.9]. In fact, given  $\boldsymbol{\eta} \in \mathbf{H}$ , we let  $z \in W^{1,p}(B)$  be the unique weak solution of the boundary value problem:

$$\Delta z = \begin{cases} \operatorname{div} \boldsymbol{\eta} & \text{in } \Omega \\ \frac{-1}{|B \setminus \overline{\Omega}|} \int_{\Omega} \operatorname{div} \boldsymbol{\eta} & \text{in } B \setminus \overline{\Omega} \end{cases}, \quad \nabla z \cdot \mathbf{n} = 0 \quad \text{on } \partial B, \quad \int_{\Omega} z = 0.$$

Since,  $B$  is a convex domain, it is well known that  $z \in W^{2,p}(B)$  (see [35, Theorem 1.1]) and

$$\|z\|_{W^{2,p}(B)} \leq c \|\operatorname{div} \boldsymbol{\eta}\|_{L^p(\Omega)},$$

where  $c > 0$  is independent of  $z$ . We let  $\boldsymbol{\xi} = (\nabla z)|_{\Omega} \in \mathbf{W}^{1,p}(\Omega)$ , and observe that  $\operatorname{div} \boldsymbol{\xi} = \Delta z = \operatorname{div} \boldsymbol{\eta}$  in  $\Omega$ ,  $\boldsymbol{\xi} \cdot \mathbf{n} = 0$  on  $\partial B$  (which certainly yields  $\boldsymbol{\xi} \cdot \mathbf{n} = 0$  on  $\Gamma_N$ ) and

$$\|\boldsymbol{\xi}\|_{\mathbf{W}^{1,p}(\Omega)} \leq c \|\operatorname{div} \boldsymbol{\eta}\|_{L^p(\Omega)}. \quad (4.4)$$

On the other hand, let  $\boldsymbol{\varepsilon} := \boldsymbol{\eta} - \boldsymbol{\xi}$ . Clearly,  $\boldsymbol{\varepsilon}$  is a divergence-free vector in  $\Omega$ , and owing to the continuous embedding  $W^{1,p}(\Omega)$  into  $L^2(\Omega)$  (see, for instance, [22, Theorem B.46]) and (4.4) we have that  $\boldsymbol{\varepsilon} \in \mathbf{L}^2(\Omega)$  and

$$\|\boldsymbol{\varepsilon}\|_{0,\Omega} \leq \widehat{c} (\|\boldsymbol{\eta}\|_{0,\Omega} + \|\boldsymbol{\xi}\|_{\mathbf{W}^{1,p}(\Omega)}) \leq \widetilde{c} \|\boldsymbol{\eta}\|_{\operatorname{div}_p;\Omega}.$$

In this way, as a consequence of [28, Chapter I, Theorem 3.1], given  $\boldsymbol{\varepsilon} \in \mathbf{L}^2(\Omega)$  satisfying  $\operatorname{div} \boldsymbol{\varepsilon} = 0$  in  $\Omega$ , and  $\Omega$  connected, there exists  $w \in H^1(\Omega)$ , such that  $\boldsymbol{\varepsilon} = \operatorname{curl} w$  in  $\Omega$ , that is,

$$\boldsymbol{\eta} - \boldsymbol{\xi} = \operatorname{curl} w \quad \text{in } \Omega. \quad (4.5)$$

In turn, noting that  $0 = (\boldsymbol{\eta} - \boldsymbol{\xi}) \cdot \mathbf{n} = (\text{curl } w) \cdot \mathbf{n} = \nabla w \cdot \mathbf{s}$  on  $\Gamma_N$ , we deduce that  $w$  is constant on  $\Gamma_N$ , and therefore  $w$  can be chosen so that  $w \in H_{\Gamma_N}^1(\Omega)$ , which proves the Helmholtz decomposition for  $d = 2$ . In turn, the equivalence between  $\|\mathbf{w}\|_{1,\Omega}$  and  $|\mathbf{w}|_{1,\Omega}$ , which is result of the generalized Poincaré inequality (see, for instance, [22, Theorem B.63]), together with (4.4), (4.5) and the continuous embedding from  $W^{1,p}(\Omega)$  into  $L^2(\Omega)$ , yield

$$\|w\|_{1,\Omega} \leq c |w|_{1,\Omega} = c \|\text{curl } w\|_{0,\Omega} \leq c (\|\boldsymbol{\eta}\|_{0,\Omega} + \|\boldsymbol{\xi}\|_{\mathbf{W}^{1,p}(\Omega)}) \leq c \|\boldsymbol{\eta}\|_{\text{div}_p,\Omega}. \quad (4.6)$$

Then, it is clear that (4.4) and (4.6) imply (4.3) and conclude the proof.  $\square$

## 5 A posteriori error analysis

In this section we derive a reliable and efficient residual-based *a posteriori* error estimator for the Galerkin scheme (3.13).

In what follows we assume that the hypothesis of Theorems 3.1 and 3.3 hold, and let  $(\boldsymbol{\sigma}, \mathbf{u}, \boldsymbol{\rho}, \theta) \in \mathbb{X}_0 \times \mathbf{M} \times \mathbf{H} \times Q$  and  $(\boldsymbol{\sigma}_h, \mathbf{u}_h, \boldsymbol{\rho}_h, \theta_h) \in \mathbb{X}_{h,0} \times \mathbf{M}_h \times \mathbf{H}_h \times Q_h$  be the unique solutions of the continuous and discrete problems (3.5) and (3.13), respectively. Then, our global *a posteriori* error estimator is defined by:

$$\Theta = \left\{ \sum_{T \in \mathcal{T}_h} \Theta_T^2 \right\}^{1/2} + \left\{ \sum_{T \in \mathcal{T}_h} \left( \|\theta_h \mathbf{g} + \text{div } \boldsymbol{\sigma}_h\|_{\mathbf{L}^{4/3}(T)}^{4/3} + \|\text{div } \boldsymbol{\rho}_h\|_{\mathbf{L}^{4/3}(T)}^{4/3} \right) \right\}^{3/4}, \quad (5.1)$$

where, for each  $T \in \mathcal{T}_h$ , the local error indicator is defined as follows:

$$\begin{aligned} \Theta_T^2 &:= h_T^{2-d/2} \left\| \nabla \mathbf{u}_h - \frac{1}{\nu} (\boldsymbol{\sigma}_h + (\mathbf{u}_h \otimes \mathbf{u}_h))^d \right\|_{0,T}^2 + h_T^2 \left\| \underline{\text{curl}} \left( \frac{1}{\nu} (\boldsymbol{\sigma}_h + (\mathbf{u}_h \otimes \mathbf{u}_h))^d \right) \right\|_{0,T}^2 \\ &+ \sum_{e \in \mathcal{E}_{h,T}(\Omega)} h_e \left\| \left[ \underline{\gamma}_* \left( \frac{1}{\nu} (\boldsymbol{\sigma}_h + (\mathbf{u}_h \otimes \mathbf{u}_h))^d \right) \right] \right\|_{0,e}^2 + \sum_{e \in \mathcal{E}_{h,T}(\Gamma)} h_e \left\| \underline{\gamma}_* \left( \frac{1}{\nu} (\boldsymbol{\sigma}_h + (\mathbf{u}_h \otimes \mathbf{u}_h))^d \right) \right\|_{0,e}^2 \\ &+ h_T^{2-d/2} \left\| \nabla \theta_h - \frac{1}{\kappa} (\boldsymbol{\rho}_h + \theta_h \mathbf{u}_h) \right\|_{0,T}^2 + h_T^2 \left\| \underline{\text{curl}} \left( \frac{1}{\kappa} (\boldsymbol{\rho}_h + \theta_h \mathbf{u}_h) \right) \right\|_{0,T}^2 + \sum_{e \in \mathcal{E}_{h,T}(\Gamma_D)} h_e^{1/2} \|\theta_D - \theta_h\|_{L^4(e)}^2 \\ &+ \sum_{e \in \mathcal{E}_{h,T}(\Omega)} h_e \left\| \left[ \underline{\gamma}_* \left( \frac{1}{\kappa} (\boldsymbol{\rho}_h + \theta_h \mathbf{u}_h) \right) \right] \right\|_{0,e}^2 + \sum_{e \in \mathcal{E}_{h,T}(\Gamma_D)} h_e \left\| \underline{\gamma}_* \left( \frac{1}{\kappa} (\boldsymbol{\rho}_h + \theta_h \mathbf{u}_h) - \nabla \theta_D \right) \right\|_{0,e}^2. \end{aligned} \quad (5.2)$$

The main goal of the present section is to establish, under suitable assumptions, the existence of positive constants  $C_{rel}$  and  $C_{eff}$ , independent of the meshsizes and the continuous and discrete solutions, such that

$$C_{eff} \Theta + \text{h.o.t.} \leq \|(\boldsymbol{\sigma}, \mathbf{u}) - (\boldsymbol{\sigma}_h, \mathbf{u}_h)\| + \|(\boldsymbol{\rho}, \theta) - (\boldsymbol{\rho}_h, \theta_h)\| \leq C_{rel} \Theta + \text{h.o.t.}, \quad (5.3)$$

where h.o.t. is a generic expression denoting one or several terms of higher order. The upper and lower bounds in (5.3), which are known as the reliability and efficiency of  $\Theta$ , are derived below in Sections 5.1 and 5.2, respectively.

## 5.1 Reliability of the a posteriori error estimator

The main result of this section is stated in the following theorem.

**Theorem 5.1** *Assume that there exists a convex domain  $B$  such that  $\Omega \subseteq B$  and  $\Gamma_N \subseteq \partial B$ . Let define  $\bar{\lambda} := \min \{\nu \hat{\gamma}_F, \kappa \gamma_T\}$  and assume further that*

$$\frac{16 C_F}{\bar{\lambda} \gamma_F \hat{\gamma}_T} \|\mathbf{g}\|_{0,\Omega} \|\theta_D\|_{1/2,\Gamma_D} \leq \frac{1}{2}, \quad (5.4)$$

where  $C_F$  is the bounding constant of  $F_T$ , and  $\gamma_F, \gamma_T$  and  $\hat{\gamma}_F, \hat{\gamma}_T$  are given in (3.10) and (3.14), respectively. Then, there exist  $C_{rel} > 0$ , independent of  $h$ , such that

$$\|(\boldsymbol{\sigma}, \mathbf{u}) - (\boldsymbol{\sigma}_h, \mathbf{u}_h)\| + \|(\boldsymbol{\rho}, \theta) - (\boldsymbol{\rho}_h, \theta_h)\| \leq C_{rel} \Theta. \quad (5.5)$$

We begin the derivation of (5.5) with the next preliminary lemma.

**Lemma 5.1** *Assume that there exists a convex domain  $B$  such that  $\Omega \subseteq B$  and  $\Gamma_N \subseteq \partial B$ . Assume further that the datum  $\theta_D$  satisfies (5.4). Finally let  $(\boldsymbol{\sigma}, \mathbf{u}, \boldsymbol{\rho}, \theta) \in \mathbb{X}_0 \times \mathbf{M} \times \mathbf{H} \times \mathbf{Q}$  and  $(\boldsymbol{\sigma}_h, \mathbf{u}_h, \boldsymbol{\rho}_h, \theta_h) \in \mathbb{X}_{h,0} \times \mathbf{M}_h \times \mathbf{H}_h \times \mathbf{Q}_h$  be the unique solutions of problems (3.5) and (3.13), respectively. Then, there exists a constant  $C > 0$ , independent of  $h$ , such that*

$$\|(\boldsymbol{\sigma}, \mathbf{u}) - (\boldsymbol{\sigma}_h, \mathbf{u}_h)\| + \|(\boldsymbol{\rho}, \theta) - (\boldsymbol{\rho}_h, \theta_h)\| \leq C \left( \sup_{\substack{(\boldsymbol{\tau}, \mathbf{v}) \in \mathbb{X}_0 \times \mathbf{M} \\ (\boldsymbol{\tau}, \mathbf{v}) \neq \mathbf{0}}} \frac{|\mathcal{R}_F(\boldsymbol{\tau}, \mathbf{v})|}{\|(\boldsymbol{\tau}, \mathbf{v})\|} + \sup_{\substack{(\boldsymbol{\eta}, \psi) \in \mathbf{H} \times \mathbf{Q} \\ (\boldsymbol{\eta}, \psi) \neq \mathbf{0}}} \frac{|\mathcal{R}_T(\boldsymbol{\eta}, \psi)|}{\|(\boldsymbol{\eta}, \psi)\|} \right), \quad (5.6)$$

where  $\mathcal{R}_F : \mathbb{X}_0 \times \mathbf{M} \rightarrow \mathbb{R}$  and  $\mathcal{R}_T : \mathbf{H} \times \mathbf{Q} \rightarrow \mathbb{R}$  are the residual functionals given by

$$\mathcal{R}_F(\boldsymbol{\tau}, \mathbf{v}) = -a_F(\boldsymbol{\sigma}_h, \boldsymbol{\tau}) - b_F(\boldsymbol{\tau}, \mathbf{u}_h) - b_F(\boldsymbol{\sigma}_h, \mathbf{v}) - c_F(\mathbf{u}_h; \mathbf{u}_h, \boldsymbol{\tau}) - d_F(\theta_h, \mathbf{v})$$

for all  $(\boldsymbol{\tau}, \mathbf{v}) \in \mathbb{X}_0 \times \mathbf{M}$ , and

$$\mathcal{R}_T(\boldsymbol{\eta}, \psi) = F_T(\boldsymbol{\eta}) - a_T(\boldsymbol{\rho}_h, \boldsymbol{\eta}) - b_T(\boldsymbol{\eta}, \theta_h) - b_T(\boldsymbol{\rho}_h, \psi) - c_T(\mathbf{u}_h; \theta_h, \boldsymbol{\eta})$$

for all  $(\boldsymbol{\eta}, \psi) \in \mathbf{H} \times \mathbf{Q}$ .

*Proof.* First, using the inf-sup condition (3.8) for the error  $(\boldsymbol{\zeta}, \mathbf{z}) = (\boldsymbol{\sigma} - \boldsymbol{\sigma}_h, \mathbf{u} - \mathbf{u}_h)$ , adding and subtracting  $c_F(\mathbf{u}_h; \mathbf{u}_h, \boldsymbol{\tau}) + d_F(\theta_h, \mathbf{v})$ , and using the first and second equations of (3.5) and the continuity of the forms  $c_F$  and  $d_F$  given by (see [13, Section 3])

$$|c_F(\mathbf{w}; \mathbf{v}, \boldsymbol{\tau})| \leq \frac{1}{\nu} \|\mathbf{w}\|_{\mathbf{M}} \|\mathbf{v}\|_{\mathbf{M}} \|\boldsymbol{\tau}\|_{\mathbb{X}}, \quad |d_F(\theta, \mathbf{v})| \leq \|\mathbf{g}\|_{0,\Omega} \|\theta\|_{\mathbf{Q}} \|\mathbf{v}\|_{\mathbf{M}},$$

we deduce that

$$\begin{aligned} \frac{\gamma_F}{2} \|(\boldsymbol{\sigma} - \boldsymbol{\sigma}_h, \mathbf{u} - \mathbf{u}_h)\| &\leq \sup_{\substack{(\boldsymbol{\tau}, \mathbf{v}) \in \mathbb{X}_0 \times \mathbf{M} \\ (\boldsymbol{\tau}, \mathbf{v}) \neq \mathbf{0}}} \frac{|\mathcal{R}_F(\boldsymbol{\tau}, \mathbf{v})|}{\|(\boldsymbol{\tau}, \mathbf{v})\|} + \sup_{\substack{\mathbf{v} \in \mathbf{M} \\ \mathbf{v} \neq \mathbf{0}}} \frac{|d_F(\theta - \theta_h, \mathbf{v})|}{\|\mathbf{v}\|_{\mathbf{M}}} + \sup_{\substack{\boldsymbol{\tau} \in \mathbb{X}_0 \\ \boldsymbol{\tau} \neq \mathbf{0}}} \frac{|c_F(\mathbf{u} - \mathbf{u}_h; \mathbf{u}_h, \boldsymbol{\tau})|}{\|\boldsymbol{\tau}\|_{\mathbb{X}}} \\ &\leq \sup_{\substack{(\boldsymbol{\tau}, \mathbf{v}) \in \mathbb{X}_0 \times \mathbf{M} \\ (\boldsymbol{\tau}, \mathbf{v}) \neq \mathbf{0}}} \frac{|\mathcal{R}_F(\boldsymbol{\tau}, \mathbf{v})|}{\|(\boldsymbol{\tau}, \mathbf{v})\|} + \|\mathbf{g}\|_{0,\Omega} \|\theta - \theta_h\|_{\mathbf{Q}} + \frac{1}{\nu} \|\mathbf{u}_h\|_{\mathbf{M}} \|\mathbf{u} - \mathbf{u}_h\|_{\mathbf{M}}. \end{aligned}$$

Then, observing that the estimate (5.4) implies

$$\frac{8 C_F}{\nu \gamma_F \widehat{\gamma}_F \widehat{\gamma}_T} \|\mathbf{g}\|_{0,\Omega} \|\theta_D\|_{1/2,\Gamma_D} \leq \frac{1}{2}, \quad (5.7)$$

and since  $\|\mathbf{u}_h\|_{\mathbf{M}} \leq \|(\boldsymbol{\sigma}_h, \mathbf{u}_h)\|$ , from (5.7) and the first estimate in (3.15), we obtain

$$\frac{\gamma_F}{4} \|(\boldsymbol{\sigma} - \boldsymbol{\sigma}_h, \mathbf{u} - \mathbf{u}_h)\| \leq \sup_{\substack{(\boldsymbol{\tau}, \mathbf{v}) \in \mathbb{X}_0 \times \mathbf{M} \\ (\boldsymbol{\tau}, \mathbf{v}) \neq \mathbf{0}}} \frac{|\mathcal{R}_F(\boldsymbol{\tau}, \mathbf{v})|}{\|(\boldsymbol{\tau}, \mathbf{v})\|} + \|\mathbf{g}\|_{0,\Omega} \|\theta - \theta_h\|_Q. \quad (5.8)$$

Similarly, from the inf-sup condition (3.9), with  $(\boldsymbol{\varsigma}, \varphi) = (\boldsymbol{\rho} - \boldsymbol{\rho}_h, \theta - \theta_h)$ , the third and fourth equations of (3.5), adding and subtracting  $c_T(\mathbf{u}_h; \theta_h, \boldsymbol{\eta})$ , and using the continuity of  $c_T$  given by (see [13, Section 3])

$$|c_T(\mathbf{w}; \psi, \boldsymbol{\eta})| \leq \frac{1}{\kappa} \|\mathbf{w}\|_{\mathbf{M}} \|\psi\|_Q \|\boldsymbol{\eta}\|_{\mathbf{H}},$$

we deduce that

$$\begin{aligned} \frac{\gamma_T}{2} \|(\boldsymbol{\rho} - \boldsymbol{\rho}_h, \theta - \theta_h)\| &\leq \sup_{\substack{(\boldsymbol{\eta}, \psi) \in \mathbf{H} \times \mathbf{Q} \\ (\boldsymbol{\eta}, \psi) \neq \mathbf{0}}} \frac{|\mathcal{R}_T(\boldsymbol{\eta}, \psi)|}{\|(\boldsymbol{\eta}, \psi)\|} + \sup_{\substack{\boldsymbol{\eta} \in \mathbf{H} \\ \boldsymbol{\eta} \neq \mathbf{0}}} \frac{|c_T(\mathbf{u} - \mathbf{u}_h; \theta_h, \boldsymbol{\eta})|}{\|\boldsymbol{\eta}\|_{\mathbf{H}}} \\ &\leq \sup_{\substack{(\boldsymbol{\eta}, \psi) \in \mathbf{H} \times \mathbf{Q} \\ (\boldsymbol{\eta}, \psi) \neq \mathbf{0}}} \frac{|\mathcal{R}_T(\boldsymbol{\eta}, \psi)|}{\|(\boldsymbol{\eta}, \psi)\|} + \frac{1}{\kappa} \|\theta_h\|_Q \|\mathbf{u} - \mathbf{u}_h\|_{\mathbf{M}}. \end{aligned} \quad (5.9)$$

Next, since  $\|\mathbf{u} - \mathbf{u}_h\|_{\mathbf{M}} \leq \|(\boldsymbol{\sigma} - \boldsymbol{\sigma}_h, \mathbf{u} - \mathbf{u}_h)\|$  and  $\|\theta_h\|_Q \leq \|(\boldsymbol{\rho}_h, \theta_h)\|$ , combining (5.8) and (5.9), and using the second inequality in (3.15), it is not difficult to see that there exist positive constants  $c_1, c_2$ , independent of  $h$ , such that

$$\begin{aligned} \|(\boldsymbol{\rho} - \boldsymbol{\rho}_h, \theta - \theta_h)\| &\leq c_1 \sup_{\substack{(\boldsymbol{\tau}, \mathbf{v}) \in \mathbb{X}_0 \times \mathbf{M} \\ (\boldsymbol{\tau}, \mathbf{v}) \neq \mathbf{0}}} \frac{|\mathcal{R}_F(\boldsymbol{\tau}, \mathbf{v})|}{\|(\boldsymbol{\tau}, \mathbf{v})\|} + c_2 \sup_{\substack{(\boldsymbol{\eta}, \psi) \in \mathbf{H} \times \mathbf{Q} \\ (\boldsymbol{\eta}, \psi) \neq \mathbf{0}}} \frac{|\mathcal{R}_T(\boldsymbol{\eta}, \psi)|}{\|(\boldsymbol{\eta}, \psi)\|} \\ &\quad + \frac{16 C_F}{\kappa \gamma_T \widehat{\gamma}_F \widehat{\gamma}_T} \|\mathbf{g}\|_{0,\Omega} \|\theta_D\|_{1/2,\Gamma_D} \|\theta - \theta_h\|_Q \end{aligned}$$

which combined with (5.4) implies

$$\|(\boldsymbol{\rho} - \boldsymbol{\rho}_h, \theta - \theta_h)\| \leq \widehat{c}_1 \sup_{\substack{(\boldsymbol{\tau}, \mathbf{v}) \in \mathbb{X}_0 \times \mathbf{M} \\ (\boldsymbol{\tau}, \mathbf{v}) \neq \mathbf{0}}} \frac{|\mathcal{R}_F(\boldsymbol{\tau}, \mathbf{v})|}{\|(\boldsymbol{\tau}, \mathbf{v})\|} + \widehat{c}_2 \sup_{\substack{(\boldsymbol{\eta}, \psi) \in \mathbf{H} \times \mathbf{Q} \\ (\boldsymbol{\eta}, \psi) \neq \mathbf{0}}} \frac{|\mathcal{R}_T(\boldsymbol{\eta}, \psi)|}{\|(\boldsymbol{\eta}, \psi)\|}, \quad (5.10)$$

with  $\widehat{c}_1, \widehat{c}_2 > 0$ , independent of  $h$ . In turn, from (5.8), (5.10) and estimate  $\|\theta - \theta_h\|_Q \leq \|(\boldsymbol{\rho} - \boldsymbol{\rho}_h, \theta - \theta_h)\|$  we easily deduce that

$$\|(\boldsymbol{\sigma} - \boldsymbol{\sigma}_h, \mathbf{u} - \mathbf{u}_h)\| \leq \widehat{c}_3 \sup_{\substack{(\boldsymbol{\tau}, \mathbf{v}) \in \mathbb{X}_0 \times \mathbf{M} \\ (\boldsymbol{\tau}, \mathbf{v}) \neq \mathbf{0}}} \frac{|\mathcal{R}_F(\boldsymbol{\tau}, \mathbf{v})|}{\|(\boldsymbol{\tau}, \mathbf{v})\|} + \widehat{c}_4 \sup_{\substack{(\boldsymbol{\eta}, \psi) \in \mathbf{H} \times \mathbf{Q} \\ (\boldsymbol{\eta}, \psi) \neq \mathbf{0}}} \frac{|\mathcal{R}_T(\boldsymbol{\eta}, \psi)|}{\|(\boldsymbol{\eta}, \psi)\|}. \quad (5.11)$$

with  $\widehat{c}_3, \widehat{c}_4 > 0$ , independent of  $h$ . In this way, estimate (5.6) follows from (5.10) and (5.11).  $\square$

Now, according to the definition of the forms  $a_F, b_F, c_F, d_F, a_T, b_T$  and  $c_T$  (c.f. (3.6)), we find that, for any  $(\boldsymbol{\tau}, \mathbf{v}) \in \mathbb{X}_0 \times \mathbf{M}$  and  $(\boldsymbol{\eta}, \psi) \in \mathbf{H} \times \mathbf{Q}$ , there holds

$$\mathcal{R}_F(\boldsymbol{\tau}, \mathbf{v}) = \mathcal{R}_{F,1}(\boldsymbol{\tau}) + \mathcal{R}_{F,2}(\mathbf{v}) \quad \text{and} \quad \mathcal{R}_T(\boldsymbol{\eta}, \psi) = \mathcal{R}_{T,1}(\boldsymbol{\eta}) + \mathcal{R}_{T,2}(\psi)$$

where

$$\mathcal{R}_{F,1}(\boldsymbol{\tau}) = -\frac{1}{\nu}(\boldsymbol{\sigma}_h^d, \boldsymbol{\tau}^d)_\Omega - (\mathbf{u}_h, \mathbf{div} \boldsymbol{\tau})_\Omega - \frac{1}{\nu} \left( (\mathbf{u}_h \otimes \mathbf{u}_h)^d, \boldsymbol{\tau} \right)_\Omega, \quad (5.12)$$

$$\mathcal{R}_{F,2}(\mathbf{v}) = -(\theta_h \mathbf{g}, \mathbf{v})_\Omega - (\mathbf{v}, \mathbf{div} \boldsymbol{\sigma}_h)_\Omega, \quad (5.13)$$

$$\mathcal{R}_{T,1}(\boldsymbol{\eta}) = \langle \boldsymbol{\eta} \cdot \mathbf{n}, \theta_D \rangle_{\Gamma_D} - \frac{1}{\kappa}(\boldsymbol{\rho}_h, \boldsymbol{\eta})_\Omega - (\theta_h, \mathbf{div} \boldsymbol{\eta})_\Omega - \frac{1}{\kappa}(\theta_h \mathbf{u}_h, \boldsymbol{\eta})_\Omega \quad (5.14)$$

and

$$\mathcal{R}_{T,2}(\psi) = -(\psi, \mathbf{div} \boldsymbol{\rho}_h)_\Omega. \quad (5.15)$$

Hence, the supremum in (5.6) can be bounded in terms of  $\mathcal{R}_{F,1}$ ,  $\mathcal{R}_{F,2}$ ,  $\mathcal{R}_{T,1}$  and  $\mathcal{R}_{T,2}$  as follows

$$\|(\boldsymbol{\sigma}, \mathbf{u}) - (\boldsymbol{\sigma}_h, \mathbf{u}_h)\| + \|(\boldsymbol{\rho}, \theta) - (\boldsymbol{\rho}_h, \theta_h)\| \leq C \left\{ \|\mathcal{R}_{F,1}\|_{\mathbb{X}'_0} + \|\mathcal{R}_{F,2}\|_{\mathbf{M}'} + \|\mathcal{R}_{T,1}\|_{\mathbf{H}'} + \|\mathcal{R}_{T,2}\|_{Q'} \right\}.$$

In this way, we have transformed (5.6) into an estimate involving global inf-sup conditions on  $\mathbb{X}_0$ ,  $\mathbf{M}$ ,  $\mathbf{H}$  and  $Q$ , separately.

Throughout the rest of this section, we provide suitable upper bounds for  $\mathcal{R}_{F,1}$ ,  $\mathcal{R}_{F,2}$ ,  $\mathcal{R}_{T,1}$  and  $\mathcal{R}_{T,2}$ . We begin by establishing the corresponding estimates for  $\mathcal{R}_{F,2}$  and  $\mathcal{R}_{T,2}$  (cf. (5.13) and (5.15)), which follow from a straightforward application of the Hölder inequality.

**Lemma 5.2** *There holds*

$$\|\mathcal{R}_{F,2}\|_{\mathbf{M}'} \leq \left\{ \sum_{T \in \mathcal{T}_h} \|\theta_h \mathbf{g} + \mathbf{div} \boldsymbol{\sigma}_h\|_{\mathbf{L}^{4/3}(T)}^{4/3} \right\}^{3/4} \quad \text{and} \quad \|\mathcal{R}_{T,2}\|_{Q'} \leq \left\{ \sum_{T \in \mathcal{T}_h} \|\mathbf{div} \boldsymbol{\rho}_h\|_{\mathbf{L}^{4/3}(T)}^{4/3} \right\}^{3/4}. \quad (5.16)$$

Note that from (5.16) and the inequality  $a^p + b^p \leq 2^{1-p}(a+b)^p$ , for all  $a, b \geq 0$  and  $0 < p \leq 1$ , we have that there exists  $C_1 > 0$  such that

$$\|\mathcal{R}_{F,2}\|_{\mathbf{M}'} + \|\mathcal{R}_{T,2}\|_{Q'} \leq C_1 \left\{ \sum_{T \in \mathcal{T}_h} \left( \|\theta_h \mathbf{g} + \mathbf{div} \boldsymbol{\sigma}_h\|_{\mathbf{L}^{4/3}(T)}^{4/3} + \|\mathbf{div} \boldsymbol{\rho}_h\|_{\mathbf{L}^{4/3}(T)}^{4/3} \right) \right\}^{3/4}.$$

In turn, after a slight modification of the proof of [9, Lemma 5.6] is it not difficult to see that the following estimate for  $\mathcal{R}_{F,1}$  (cf. (5.12)) holds.

**Lemma 5.3** *There exists  $C_2 > 0$ , independent of  $h$ , such that*

$$\|\mathcal{R}_{F,1}\|_{\mathbb{X}'_0} \leq C_2 \left\{ \sum_{T \in \mathcal{T}_h} \Theta_{1,T}^2 \right\}^{1/2},$$

where

$$\begin{aligned} \Theta_{1,T}^2 &:= h_T^{2-d/2} \left\| \nabla \mathbf{u}_h - \frac{1}{\nu}(\boldsymbol{\sigma}_h + (\mathbf{u}_h \otimes \mathbf{u}_h))^d \right\|_{0,T}^2 + h_T^2 \left\| \underline{\mathbf{curl}} \left( \frac{1}{\nu}(\boldsymbol{\sigma}_h + (\mathbf{u}_h \otimes \mathbf{u}_h))^d \right) \right\|_{0,T}^2 \\ &+ \sum_{e \in \mathcal{E}_{h,T}(\Omega)} h_e \left\| \left[ \left[ \gamma_* \left( \frac{1}{\nu}(\boldsymbol{\sigma}_h + (\mathbf{u}_h \otimes \mathbf{u}_h))^d \right) \right] \right]_{0,e} \right\|^2 + \sum_{e \in \mathcal{E}_{h,T}(\Gamma)} h_e \left\| \gamma_* \left( \frac{1}{\nu}(\boldsymbol{\sigma}_h + (\mathbf{u}_h \otimes \mathbf{u}_h))^d \right) \right\|_{0,e}^2. \end{aligned}$$

Our next goal is to bound the remaining term  $\|\mathcal{R}_{T,1}\|_{\mathbf{H}'}$ . To do that we need to introduce the following two technical results.



**Lemma 5.4** *There exists  $C_3 > 0$ , independent of  $h$ , such that for each  $\boldsymbol{\xi} \in \mathbf{W}^{1,4/3}(\Omega)$  there holds*

$$|\mathcal{R}_{T,1}(\boldsymbol{\xi} - \Pi_h^k(\boldsymbol{\xi}))| \leq C_3 \left\{ \sum_{T \in \mathcal{T}_h} \Theta_{2,T}^2 \right\}^{1/2} \|\boldsymbol{\xi}\|_{\mathbf{W}^{1,4/3}(\Omega)}, \quad (5.17)$$

where

$$\Theta_{2,T}^2 := h_T^{2-d/2} \left\| \nabla \theta_h - \frac{1}{\kappa}(\boldsymbol{\rho}_h + \theta_h \mathbf{u}_h) \right\|_{0,T}^2 + \sum_{e \in \mathcal{E}_{h,T}(\Gamma_D)} h_e^{1/2} \|\theta_D - \theta_h\|_{L^4(e)}^2. \quad (5.18)$$

*Proof.* We recall from the definition of  $\mathcal{R}_{T,1}$  (cf. (5.14)) that

$$\begin{aligned} \mathcal{R}_{T,1}(\boldsymbol{\xi} - \Pi_h^k(\boldsymbol{\xi})) &= \langle (\boldsymbol{\xi} - \Pi_h^k(\boldsymbol{\xi})) \mathbf{n}, \theta_D \rangle_{\Gamma_D} - \frac{1}{\kappa} \left( \boldsymbol{\rho}_h, \boldsymbol{\xi} - \Pi_h^k(\boldsymbol{\xi}) \right)_{\Omega} \\ &\quad - \left( \theta_h, \operatorname{div}(\boldsymbol{\xi} - \Pi_h^k(\boldsymbol{\xi})) \right)_{\Omega} - \frac{1}{\kappa} \left( \theta_h \mathbf{u}_h, \boldsymbol{\xi} - \Pi_h^k(\boldsymbol{\xi}) \right). \end{aligned}$$

Then, similarly to [9, Lemma 5.3], applying a local integration by parts to the third term above, using (4.1) and the fact that  $\theta_D \in L^2(\Gamma_D)$ , we obtain

$$\mathcal{R}_{T,1}(\boldsymbol{\xi} - \Pi_h^k(\boldsymbol{\xi})) = \sum_{T \in \mathcal{T}_h} \left( \nabla \theta_h - \frac{1}{\kappa}(\boldsymbol{\rho}_h + \theta_h \mathbf{u}_h), (\boldsymbol{\xi} - \Pi_h^k(\boldsymbol{\xi})) \right)_T + \sum_{e \in \mathcal{E}_h(\Gamma_D)} \left( (\boldsymbol{\xi} - \Pi_h^k(\boldsymbol{\xi})) \mathbf{n}, \theta_D - \theta_h \right)_e.$$

In turn, using the Hölder and Cauchy-Schwarz inequalities, the interpolation property (4.2) with  $p = 4/3$ , and the fact that there exists a positive constant  $C > 0$  independent of the mesh, such that

$$\|\tau - \Pi_h^k(\tau)\|_{0,T} \leq C h_T^{1-d/4} |\tau|_{\mathbf{W}^{1,4/3}(T)} \quad \forall \tau \in \mathbf{W}^{1,4/3}(T),$$

whose proof follows from Lemma 4.1 and [10, Remark 4.2], we deduce that

$$\begin{aligned} |\mathcal{R}_{T,1}(\boldsymbol{\xi} - \Pi_h^k(\boldsymbol{\xi}))| &\leq \sum_{T \in \mathcal{T}_h} \left\| \nabla \theta_h - \frac{1}{\kappa}(\boldsymbol{\rho}_h + \theta_h \mathbf{u}_h) \right\|_{0,T} C h_T^{1-d/4} |\boldsymbol{\xi}|_{\mathbf{W}^{1,4/3}(T)} \\ &\quad + \sum_{e \in \mathcal{E}_h(\Gamma_D)} \|\theta_D - \theta_h\|_{L^4(e)} C h_e^{1/4} |\boldsymbol{\xi}|_{\mathbf{W}^{1,4/3}(T_e)}, \end{aligned}$$

with  $T_e$  being the element containing  $e$ . Next, by using the Cauchy-Schwarz and subadditivity inequalities and the fact that we are considering regular meshes, we obtain

$$\begin{aligned} |\mathcal{R}_{T,1}(\boldsymbol{\xi} - \Pi_h^k(\boldsymbol{\xi}))| &\leq \widehat{C} \left\{ \left( \sum_{T \in \mathcal{T}_h} h_T^{2-d/2} \left\| \nabla \theta_h - \frac{1}{\kappa}(\boldsymbol{\rho}_h + \theta_h \mathbf{u}_h) \right\|_{0,T}^2 \right)^{1/2} \left( \sum_{T \in \mathcal{T}_h} |\boldsymbol{\xi}|_{\mathbf{W}^{1,4/3}(T)}^{4/3} \right)^{3/4} \right. \\ &\quad \left. + \left( \sum_{e \in \mathcal{E}_h(\Gamma_D)} h_e^{1/2} \|\theta_D - \theta_h\|_{L^4(e)}^2 \right)^{1/2} \left( \sum_{e \in \mathcal{E}_h(\Gamma_D)} |\boldsymbol{\xi}|_{\mathbf{W}^{1,4/3}(T_e)}^{4/3} \right)^{3/4} \right\}, \end{aligned}$$

which clearly implies (5.17) and completes the proof.  $\square$

**Lemma 5.5** *Assume that  $\theta_D \in H^1(\Gamma_D)$  and let*

$$\begin{aligned} \Theta_{3,T}^2 &:= h_T^2 \left\| \operatorname{curl} \left( \frac{1}{\kappa}(\boldsymbol{\rho}_h + \theta_h \mathbf{u}_h) \right) \right\|_{0,T}^2 + \sum_{e \in \mathcal{E}_{h,T}(\Omega)} h_e \left\| \left[ \left[ \gamma_* \left( \frac{1}{\kappa}(\boldsymbol{\rho}_h + \theta_h \mathbf{u}_h) \right) \right] \right] \right\|_{0,e}^2 \\ &\quad + \sum_{e \in \mathcal{E}_{h,T}(\Gamma_D)} h_e \left\| \gamma_* \left( \frac{1}{\kappa}(\boldsymbol{\rho}_h + \theta_h \mathbf{u}_h) - \nabla \theta_D \right) \right\|_{0,e}^2. \end{aligned} \quad (5.19)$$

a) Let  $w \in \mathbf{H}_{\Gamma_N}^1(\Omega)$  and  $d = 2$ . Then, there exists  $C_4 > 0$ , independent of  $h$ , such that

$$|\mathcal{R}_{T,1}(\operatorname{curl}(w - I_h w))| \leq C_4 \left\{ \sum_{T \in \mathcal{T}_h} \Theta_{3,T}^2 \right\}^{1/2} \|w\|_{1,\Omega} \quad (5.20)$$

b) Let  $\mathbf{w} \in \mathbf{H}_{\Gamma_N}^1(\Omega)$  and  $d = 3$ . Then, there exists  $\widehat{C}_4 > 0$ , independent of  $h$ , such that

$$|\mathcal{R}_{T,1}(\mathbf{curl}(\mathbf{w} - \mathbf{I}_h \mathbf{w}))| \leq \widehat{C}_4 \left\{ \sum_{T \in \mathcal{T}_h} \Theta_{3,T}^2 \right\}^{1/2} \|\mathbf{w}\|_{1,\Omega}.$$

*Proof.* In what follows we prove the result for the two-dimensional case since for the three dimensional case follows analogously.

We proceed as in [9, Lemma 5.5]. In fact, given  $w \in \mathbf{H}^1(\Omega)$ , we first notice from the definition of  $\mathcal{R}_{T,1}$  in (5.14) that there holds

$$\mathcal{R}_{T,1}(\operatorname{curl}(w - I_h w)) = \langle \operatorname{curl}(w - I_h w) \cdot \mathbf{n}, \theta_D \rangle_{\Gamma_D} - \frac{1}{\kappa} (\boldsymbol{\rho}_h + \theta_h \mathbf{u}_h, \operatorname{curl}(w - I_h w))_{\Omega}.$$

Recalling that  $\theta_D \in \mathbf{H}^1(\Gamma_D)$ , now we apply the following integration by parts on the boundary  $\Gamma_D$  given by (see, for instance, [21, Lemma 3.5, eq. (3.34)])

$$\langle \operatorname{curl}(w - I_h w) \cdot \mathbf{n}, \theta_D \rangle_{\Gamma_D} = \langle \nabla \theta_D \cdot \mathbf{s}, w - I_h w \rangle_{\Gamma_D} = \langle \gamma_*(\nabla \theta_D), w - I_h w \rangle_{\Gamma_D},$$

which together with a local integration by parts, the fact that  $w|_{\Gamma_N} = I_h w|_{\Gamma_N} = 0$  and noting that  $\gamma_*(\nabla \theta_D) \in \mathbf{L}^2(\Gamma_D)$ , allow us to deduce that

$$\begin{aligned} \mathcal{R}_{T,1}(\operatorname{curl}(w - I_h w)) &= - \sum_{T \in \mathcal{T}_h} \left( \underline{\operatorname{curl}} \left( \frac{1}{\kappa} (\boldsymbol{\rho}_h + \theta_h \mathbf{u}_h) \right), w - I_h w \right)_T \\ &+ \sum_{e \in \mathcal{E}_h(\Omega)} \left( \left[ \left[ \gamma_* \left( \frac{1}{\kappa} (\boldsymbol{\rho}_h + \theta_h \mathbf{u}_h) \right) \right] \right], w - I_h w \right)_e \\ &+ \sum_{e \in \mathcal{E}_h(\Gamma_D)} \left( \gamma_* \left( \frac{1}{\kappa} (\boldsymbol{\rho}_h + \theta_h \mathbf{u}_h) - \nabla \theta_D \right), w - I_h w \right)_e. \end{aligned}$$

Hence, applying Cauchy-Schwarz inequality and the approximation properties of the Cl  ment interpolant (cf. Lemma 4.3), we obtain

$$\begin{aligned} &|\mathcal{R}_{T,1}(\operatorname{curl}(w - I_h w))| \\ &\leq \widehat{C} \left\{ \left( \sum_{T \in \mathcal{T}_h} h_T^2 \left\| \underline{\operatorname{curl}} \left( \frac{1}{\kappa} (\boldsymbol{\rho}_h + \theta_h \mathbf{u}_h) \right) \right\|_{0,T}^2 \right)^{1/2} \left( \sum_{T \in \mathcal{T}_h} \|w\|_{1,\Delta(T)}^2 \right)^{1/2} \right. \\ &+ \left( \sum_{e \in \mathcal{E}_h(\Omega)} h_e \left\| \left[ \left[ \gamma_* \left( \frac{1}{\kappa} (\boldsymbol{\rho}_h + \theta_h \mathbf{u}_h) \right) \right] \right] \right\|_{0,e}^2 \right)^{1/2} \left( \sum_{e \in \mathcal{E}_h(\Omega)} \|w\|_{1,\Delta(e)}^2 \right)^{1/2} \\ &\left. + \left( \sum_{e \in \mathcal{E}_h(\Gamma_D)} h_e \left\| \gamma_* \left( \frac{1}{\kappa} (\boldsymbol{\rho}_h + \theta_h \mathbf{u}_h) - \nabla \theta_D \right) \right\|_{0,e}^2 \right)^{1/2} \left( \sum_{e \in \mathcal{E}_h(\Gamma_D)} \|w\|_{1,\Delta(e)}^2 \right)^{1/2} \right\}. \end{aligned}$$

Therefore, as a direct consequence of the previous estimate and the fact that the number of triangles of the macro-elements  $\Delta(T)$  and  $\Delta(e)$  are uniformly bounded, we get (5.20) concluding the proof.  $\square$

The following lemma establishes the estimate for  $\mathcal{R}_{T,1}$ .

**Lemma 5.6** *There exists  $C_5 > 0$ , independent of  $h$ , such that*

$$\|\mathcal{R}_{T,1}\|_{\mathbb{X}'_0} \leq C_5 \left\{ \sum_{T \in \mathcal{T}_h} (\Theta_{2,T}^2 + \Theta_{3,T}^2) \right\}^{1/2},$$

with  $\Theta_{2,T}$  and  $\Theta_{3,T}$  defined as in (5.18) and (5.19) respectively.

*Proof.* For simplicity, we prove the result for the two-dimensional case. The three dimensional case follows analogously.

Let  $\boldsymbol{\eta} \in \mathbf{H}$ . It follows from Lemma 4.4 that there exist  $\boldsymbol{\xi} \in \mathbf{W}^{1,4/3}(\Omega)$  and  $w \in H_{\Gamma_N}^1(\Omega)$ , such that  $\boldsymbol{\eta} = \boldsymbol{\xi} + \text{curl } w$  and

$$\|\boldsymbol{\xi}\|_{\mathbf{W}^{1,4/3}(\Omega)} + \|w\|_{1,\Omega} \leq C_{Hel} \|\boldsymbol{\eta}\|_{\mathbf{H}}. \quad (5.21)$$

Notice from the Galerkin scheme (3.13) that  $\mathcal{R}_{T,1}(\boldsymbol{\eta}_h) = 0$  for all  $\boldsymbol{\eta}_h \in \mathbf{H}_h$ . Hence,

$$\mathcal{R}_{T,1}(\boldsymbol{\eta}) = \mathcal{R}_{T,1}(\boldsymbol{\eta} - \boldsymbol{\eta}_h) \quad \forall \boldsymbol{\eta}_h \in \mathbf{H}_h.$$

In particular, for  $\boldsymbol{\eta}_h$  defined as

$$\boldsymbol{\eta}_h = \Pi_h^k \boldsymbol{\xi} + \text{curl}(I_h w),$$

whence

$$\mathcal{R}_{T,1}(\boldsymbol{\eta}) = \mathcal{R}_{T,1}(\boldsymbol{\xi} - \Pi_h^k \boldsymbol{\xi}) + \mathcal{R}_{T,1}(\text{curl}(w - I_h w)).$$

Hence, the proof follows from Lemmas 5.4 and 5.5, and estimate (5.21).  $\square$

We end this section by observing that the reliability estimate (5.5) is a direct consequence of Lemmas 5.1, 5.2, 5.3 and 5.6.

## 5.2 Efficiency of the a posteriori error estimator

The main result of this section is stated as follows.

**Theorem 5.2** *There exists  $C_{eff} > 0$ , independent of  $h$ , such that*

$$C_{eff} \Theta \leq \|(\boldsymbol{\sigma}, \mathbf{u}) - (\boldsymbol{\sigma}_h, \mathbf{u}_h)\| + \|(\boldsymbol{\rho}, \theta) - (\boldsymbol{\rho}_h, \theta_h)\| + \text{h.o.t.}, \quad (5.22)$$

where h.o.t. stands for one or several terms of higher order.

We remark in advance that the proof of (5.22) makes frequent use of the identities provided by Theorem 3.2. We begin with the estimates for the zero order terms appearing in the definition of  $\Theta_T$  (cf. (5.2)).

**Lemma 5.7** *For all  $T \in \mathcal{T}_h$  there holds*

$$\|\theta_h \mathbf{g} + \text{div} \boldsymbol{\sigma}_h\|_{\mathbf{L}^{4/3}(T)} \leq \|\boldsymbol{\sigma} - \boldsymbol{\sigma}_h\|_{\text{div}_{4/3;T}} + \|\mathbf{g}\|_{0,\Omega} \|\theta - \theta_h\|_{L^4(T)}$$

and

$$\|\text{div} \boldsymbol{\rho}_h\|_{L^{4/3}(T)} \leq \|\boldsymbol{\rho} - \boldsymbol{\rho}_h\|_{\text{div}_{4/3;T}}.$$

*Proof.* It suffices to recall, as established in Theorem 3.2, that  $\mathbf{div} \boldsymbol{\sigma} + \theta \mathbf{g} = \mathbf{0}$  and  $\mathbf{div} \boldsymbol{\rho} = 0$  in  $\Omega$ .  $\square$

In order to derive the upper bounds for the remaining terms defining the global *a posteriori* error estimator  $\Theta$  (cf. (5.1)), we use results from [11], inverse inequalities, and the localization technique based on element-bubble and edge-bubble functions. To this end, we now introduce further notations and preliminary results. Given  $T \in \mathcal{T}_h$  and  $e \in \mathcal{E}_{h,T}$ , we let  $\phi_T$  and  $\phi_e$  be the usual element-bubble and edge-bubble functions, respectively (see [37] for details). In particular  $\phi_T$  satisfies  $\phi_T \in P_3(T)$ ,  $\text{supp } \phi_T \subseteq T$ ,  $\phi_T = 0$  on  $\partial T$ , and  $0 \leq \phi_T \leq 1$  in  $T$ . Similarly,  $\phi_e|_T \in P_2(T)$ ,  $\text{supp } \phi_e \subseteq \omega_e := \cup\{T' \in \mathcal{T}_h : e \in \mathcal{E}_{h,T'}\}$ ,  $\phi_e = 0$  on  $\partial T \setminus e$  and  $0 \leq \phi_e \leq 1$  in  $\omega_e$ . We also recall from [36] that, given  $k \in \mathbb{N} \cup \{0\}$ , there exists an extension operator  $L : C(e) \rightarrow C(\omega_e)$  that satisfies  $L(p) \in P_k(T)$  and  $L(p)|_e = p \forall p \in P_k(e)$ . A corresponding vector version of  $L$ , that is the componentwise application of  $L$ , is denoted by  $\mathbf{L}$ . Additional properties of  $\phi_T$ ,  $\phi_e$  and  $L$  are collected in the following lemma.

**Lemma 5.8** *Given  $k \in \mathbb{N} \cup \{0\}$ , there exist positive constants  $c_1, c_2, c_3$  and  $c_4$ , depending only on  $k$  and the shape regularity of the triangulations (minimum angle condition), such that, for each triangle  $T$  and  $e \in \mathcal{E}_h$ , there hold*

$$\|\phi_T q\|_{0,T}^2 \leq \|q\|_{0,T}^2 \leq c_1 \|\phi_T^{1/2} q\|_{0,T}^2 \quad \forall q \in P_k(T), \quad (5.23)$$

$$\|\phi_e L(p)\|_{0,e}^2 \leq \|p\|_{0,e}^2 \leq c_2 \|\phi_e^{1/2} p\|_{0,e}^2 \quad \forall p \in P_k(e)$$

and

$$c_3 h_e^{1/2} \|p\|_{0,e} \leq \|\phi_e^{1/2} L(p)\|_{0,T} \leq c_4 h_e^{1/2} \|p\|_{0,e} \quad \forall p \in P_k(e).$$

*Proof.* See Lemma 1.3 in [36].  $\square$

In addition, given  $k \in \mathbb{N} \cup \{0\}$ ,  $T \in \mathcal{T}_h$  and  $e \in \mathcal{E}_h$ , in what follows we will make use of the following inverse inequalities (see [22, Lemma 1.138]): There exist  $c_1, c_2 > 0$ , independent of the meshsize, such that

$$\|v\|_{W^{1,4/3}(T)} \leq c_1 h_T^{-1+d/4} \|v\|_{0,T} \quad \forall v \in P_k(T), \quad (5.24)$$

$$\|v\|_{L^4(e)} \leq c_2 h_e^{(1-d)/4} \|v\|_{0,e} \quad \forall v \in P_k(e). \quad (5.25)$$

Finally, we recall a discrete trace inequality, which establishes the existence of a positive constant  $c$ , depending only on the shape regularity of the triangulations, such that for each  $T \in \mathcal{T}_h$  and  $e \in \mathcal{E}_{h,T}$ , there holds

$$\|v\|_{0,e}^2 \leq c (h_e^{-1} \|v\|_{0,T}^2 + h_e |v|_{1,T}^2) \quad \forall v \in H^1(T). \quad (5.26)$$

For the proof of inequality (5.26) we refer to Theorem 3.10 in [1].

The corresponding bounds for the remaining terms defining  $\Theta_{1,T}$  are stated in the following lemmas.

**Lemma 5.9** *There exists  $C_1 > 0$ , independent of  $h$ , such that*

$$\begin{aligned} & h_T^{1-d/4} \left\| \nabla \mathbf{u}_h - \frac{1}{\nu} (\boldsymbol{\sigma}_h + (\mathbf{u}_h \otimes \mathbf{u}_h))^d \right\|_{0,T} \\ & \leq C_1 \left\{ (1 + h_T^{1-d/4}) \|\mathbf{u} - \mathbf{u}_h\|_{L^4(T)} + h_T^{1-d/4} \|\boldsymbol{\sigma} - \boldsymbol{\sigma}_h\|_{0,T} \right\} \quad \forall T \in \mathcal{T}_h. \end{aligned}$$

*Proof.* See Lemma 5.10 in [9].  $\square$

**Lemma 5.10** *There exist  $C_2 > 0$ ,  $C_3 > 0$  and  $C_4 > 0$ , independent of  $h$ , such that*

$$h_T \left\| \underline{\text{curl}} \left( \frac{1}{\nu} (\boldsymbol{\sigma}_h + (\mathbf{u}_h \otimes \mathbf{u}_h))^{\text{d}} \right) \right\|_{0,T} \leq C_2 \left\{ \|\mathbf{u} - \mathbf{u}_h\|_{\mathbf{L}^4(T)} + \|\boldsymbol{\sigma} - \boldsymbol{\sigma}_h\|_{0,T} \right\}$$

for all  $T \in \mathcal{T}_h$ ,

$$h_e^{1/2} \left\| \left[ \left[ \underline{\gamma}_* \left( \frac{1}{\nu} (\boldsymbol{\sigma}_h + (\mathbf{u}_h \otimes \mathbf{u}_h))^{\text{d}} \right) \right] \right] \right\|_{0,e} \leq C_3 \left\{ \|\mathbf{u} - \mathbf{u}_h\|_{\mathbf{L}^4(\omega_e)} + \|\boldsymbol{\sigma} - \boldsymbol{\sigma}_h\|_{0,\omega_e} \right\}$$

for all  $e \in \mathcal{E}_h(\Omega)$ , and

$$h_e^{1/2} \left\| \underline{\gamma}_* \left( \frac{1}{\nu} (\boldsymbol{\sigma}_h + (\mathbf{u}_h \otimes \mathbf{u}_h))^{\text{d}} \right) \right\|_{0,e} \leq C_4 \left\{ \|\mathbf{u} - \mathbf{u}_h\|_{\mathbf{L}^4(T_e)} + \|\boldsymbol{\sigma} - \boldsymbol{\sigma}_h\|_{0,T_e} \right\}$$

for all  $e \in \mathcal{E}_h(\Gamma)$ , where  $T_e$  is the element to which the boundary edge or boundary face  $e$  belongs.

*Proof.* It follows from Lemma 5.12 in [9] with  $\mathbf{u}_D = \mathbf{0}$  on  $\Gamma$ . □

Now, we aim to provide upper bounds for the terms defining  $\Theta_{2,T}$ .

**Lemma 5.11** *There exists  $C_5 > 0$ , independent of  $h$ , such that*

$$\begin{aligned} & h_T^{1-d/4} \left\| \nabla \theta_h - \frac{1}{\kappa} (\boldsymbol{\rho}_h + \theta_h \mathbf{u}_h) \right\|_{0,T} \\ & \leq C_5 \left\{ (1 + h_T^{1-d/4}) \|\theta - \theta_h\|_{\mathbf{L}^4(T)} + h_T^{1-d/4} \|\boldsymbol{\rho} - \boldsymbol{\rho}_h\|_{0,T} + h_T^{1-d/4} \|\mathbf{u} - \mathbf{u}_h\|_{\mathbf{L}^4(T)} \right\}, \end{aligned} \quad (5.27)$$

for all  $T \in \mathcal{T}_h$ .

*Proof.* We proceed as in [9, Lemma 5.10]. In fact, given  $T \in \mathcal{T}_h$ , we define  $\boldsymbol{\chi}_T := \nabla \theta_h - \frac{1}{\kappa} (\boldsymbol{\rho}_h + \theta_h \mathbf{u}_h)$  in  $T$ . Then, applying (5.23) to  $\|\boldsymbol{\chi}_T\|_{0,T}$ , recalling the identity  $\nabla \theta = \frac{1}{\kappa} (\boldsymbol{\rho} + \theta \mathbf{u})$  in  $\Omega$  (cf. Theorem 3.2), integrating by parts and using that  $\phi_T = 0$  on  $\partial T$ , we deduce

$$\begin{aligned} \|\boldsymbol{\chi}_T\|_{0,T}^2 & \leq \|\phi_T^{1/2} \boldsymbol{\chi}_T\|_{0,T}^2 \\ & = (\text{div}(\phi_T \boldsymbol{\chi}_T), \theta - \theta_h)_T + \frac{1}{\kappa} (\phi_T \boldsymbol{\chi}_T, (\boldsymbol{\rho} - \boldsymbol{\rho}_h) + (\theta \mathbf{u} - \theta_h \mathbf{u}_h))_T. \end{aligned}$$

Next, using the Hölder and Cauchy–Schwarz inequalities, the estimates (5.24) and (5.23), we obtain

$$\begin{aligned} \|\boldsymbol{\chi}_T\|_{0,T}^2 & \leq |\phi_T \boldsymbol{\chi}_T|_{\mathbf{W}^{1,4/3}(T)} \|\theta - \theta_h\|_{\mathbf{L}^4(T)} + \frac{1}{\kappa} \|\phi_T \boldsymbol{\chi}_T\|_{0,T} \|\boldsymbol{\rho} - \boldsymbol{\rho}_h + \theta \mathbf{u} - \theta_h \mathbf{u}_h\|_{0,T} \\ & \leq C h_T^{-1+d/4} \|\boldsymbol{\chi}_T\|_{0,T} \|\theta - \theta_h\|_{\mathbf{L}^4(T)} + \frac{1}{\kappa} \|\boldsymbol{\chi}_T\|_{0,T} (\|\boldsymbol{\rho} - \boldsymbol{\rho}_h\|_{0,T} + \|\theta \mathbf{u} - \theta_h \mathbf{u}_h\|_{0,T}), \end{aligned}$$

which implies

$$\|\boldsymbol{\chi}_T\|_{0,T} \leq C h_T^{-1+d/4} \|\theta - \theta_h\|_{\mathbf{L}^4(T)} + \frac{1}{\kappa} (\|\boldsymbol{\rho} - \boldsymbol{\rho}_h\|_{0,T} + \|\theta \mathbf{u} - \theta_h \mathbf{u}_h\|_{0,T}). \quad (5.28)$$

In turn, adding and subtracting  $\theta \mathbf{u}_h$  (it also works with  $\theta_h \mathbf{u}$ ), using the Cauchy–Schwarz inequality and the fact that  $\|\theta\|_{\mathbf{L}^4(\Omega)}$  and  $\|\mathbf{u}_h\|_{\mathbf{L}^4(\Omega)}$  are bounded by data and constants, all of them independent of  $h$  (cf. (3.11) and (3.15)), we deduce that

$$\begin{aligned} \|\theta \mathbf{u} - \theta_h \mathbf{u}_h\|_{0,T} &= \|\theta(\mathbf{u} - \mathbf{u}_h) + (\theta - \theta_h) \mathbf{u}_h\|_{0,T} \\ &\leq \|\theta\|_{\mathbf{L}^4(T)} \|\mathbf{u} - \mathbf{u}_h\|_{\mathbf{L}^4(T)} + \|\mathbf{u}_h\|_{\mathbf{L}^4(T)} \|\theta - \theta_h\|_{\mathbf{L}^4(T)} \\ &\leq C \left( \|\mathbf{u} - \mathbf{u}_h\|_{\mathbf{L}^4(T)} + \|\theta - \theta_h\|_{\mathbf{L}^4(T)} \right), \end{aligned} \quad (5.29)$$

with  $C > 0$  independent of  $h$ . Finally, replacing back (5.29) into (5.28) we derive (5.27) and conclude the proof.  $\square$

**Lemma 5.12** *Suppose that  $\theta_D$  is piecewise polinomial. Then, there exists  $C_2 > 0$ , independent of  $h$ , such that*

$$h_e^{1/4} \|\theta_D - \theta_h\|_{\mathbf{L}^4(e)} \leq C_6 \left\{ (1 + h_T^{1-d/4}) \|\theta - \theta_h\|_{\mathbf{L}^4(T)} + h_T^{1-d/4} \|\boldsymbol{\rho} - \boldsymbol{\rho}_h\|_{0,T} + h_T^{1-d/4} \|\mathbf{u} - \mathbf{u}_h\|_{\mathbf{L}^4(T)} \right\} \quad (5.30)$$

for all  $e \in \mathcal{E}_{h,T}(\Gamma_D)$ .

*Proof.* We proceed as in [9, Lemma 5.11]. In fact, given  $e \in \mathcal{E}_h(\Gamma_D)$  an edge or face of an element depending on whether  $d = 2$  or  $d = 3$ , respectively. From (5.25), it follows that

$$\|\theta_D - \theta_h\|_{\mathbf{L}^4(e)} \leq C h_e^{(1-d)/4} \|\theta_D - \theta_h\|_{0,e}. \quad (5.31)$$

Hence, from (5.31) and (5.26), we deduce that

$$\|\theta_D - \theta_h\|_{\mathbf{L}^4(e)} \leq C \left\{ h_e^{(-1-d)/4} \|\theta - \theta_h\|_{0,T} + h_e^{(3-d)/4} |\theta - \theta_h|_{1,T} \right\}. \quad (5.32)$$

Next, we focus on estimating the right-hand side of (5.32). To that end, we use first the Cauchy–Schwarz inequality and the fact that for regular triangulations  $|T| \cong h_T^d$ , to deduce that there exists  $c > 0$ , independent of  $h$ , such that

$$\|\theta - \theta_h\|_{0,T} \leq c h_T^{d/4} \|\theta - \theta_h\|_{\mathbf{L}^4(T)}. \quad (5.33)$$

In turn, using the identity  $\nabla \theta = \frac{1}{\kappa}(\boldsymbol{\rho} + \theta \mathbf{u})$  in  $\Omega$  (cf. Theorem 3.2) and some algebraic computations, we deduce that

$$\begin{aligned} |\theta - \theta_h|_{1,T} &= \left\| \frac{1}{\kappa}(\boldsymbol{\rho} - \boldsymbol{\rho}_h) + \frac{1}{\kappa}(\theta \mathbf{u} - \theta_h \mathbf{u}_h) + \frac{1}{\kappa}(\boldsymbol{\rho}_h + \theta_h \mathbf{u}_h) - \nabla \theta_h \right\|_{0,T} \\ &\leq \frac{1}{\kappa} \left( \|\boldsymbol{\rho} - \boldsymbol{\rho}_h\|_{0,T} + \|\theta \mathbf{u} - \theta_h \mathbf{u}_h\|_{0,T} \right) + \left\| \nabla \theta_h - \frac{1}{\kappa}(\boldsymbol{\rho}_h + \theta_h \mathbf{u}_h) \right\|_{0,T} \end{aligned}$$

which together with (5.28) and (5.29), yields,

$$|\theta - \theta_h|_{1,T} \leq C \left\{ (1 + h_T^{-1+d/4}) \|\theta - \theta_h\|_{\mathbf{L}^4(T)} + \|\boldsymbol{\rho} - \boldsymbol{\rho}_h\|_{0,T} + \|\mathbf{u} - \mathbf{u}_h\|_{\mathbf{L}^4(T)} \right\}. \quad (5.34)$$

Therefore, (5.30) follows from estimates (5.32), (5.33) and (5.34), and the fact that  $h_e \leq h_T$ .  $\square$

**Lemma 5.13** *There exist  $C_7 > 0$  and  $C_8 > 0$ , independent of  $h$ , such that*

$$h_T \left\| \underline{\text{curl}} \left( \frac{1}{\kappa} (\boldsymbol{\rho}_h + \theta_h \mathbf{u}_h) \right) \right\|_{0,T} \leq C_7 \left\{ \|\mathbf{u} - \mathbf{u}_h\|_{\mathbf{L}^4(T)} + \|\boldsymbol{\rho} - \boldsymbol{\rho}_h\|_{0,T} + \|\theta - \theta_h\|_{\mathbf{L}^4(T)} \right\} \quad (5.35)$$

for all  $T \in \mathcal{T}_h$  and

$$h_e^{1/2} \left\| \left[ \left[ \gamma_* \left( \frac{1}{\kappa} (\boldsymbol{\rho}_h + \theta_h \mathbf{u}_h) \right) \right] \right] \right\|_{0,e} \leq C_8 \left\{ \|\mathbf{u} - \mathbf{u}_h\|_{\mathbf{L}^4(\omega_e)} + \|\boldsymbol{\rho} - \boldsymbol{\rho}_h\|_{0,\omega_e} + \|\theta - \theta_h\|_{\mathbf{L}^4(\omega_e)} \right\} \quad (5.36)$$

for all  $e \in \mathcal{E}_h(\Omega)$ .

Additionally, if  $\theta_D$  is piecewise polynomial, there exists  $C_9 > 0$ , independent of  $h$ , such that

$$h_e^{1/2} \left\| \gamma_* \left( \frac{1}{\kappa} (\boldsymbol{\rho}_h + \theta_h \mathbf{u}_h) - \nabla \theta_D \right) \right\|_{0,e} \leq C_9 \left\{ \|\mathbf{u} - \mathbf{u}_h\|_{\mathbf{L}^4(T_e)} + \|\boldsymbol{\rho} - \boldsymbol{\rho}_h\|_{0,T_e} + \|\theta - \theta_h\|_{\mathbf{L}^4(T_e)} \right\} \quad (5.37)$$

for all  $e \in \mathcal{E}_h(\Gamma)$ , where  $T_e$  is the element to which the boundary edge or boundary face  $e$  belongs.

*Proof.* For the two-dimensional case, the derivation of the first two inequalities, follows as in [17, Lemma 3.11], that is, it suffices to use Lemmas 6.1 and 6.2 in [11]. Indeed, from there we have that for each piecewise polynomial  $\boldsymbol{\eta}_h$  in  $\mathcal{T}_h$  and for each  $\boldsymbol{\eta} \in \mathbf{L}^2(\Omega)$  with  $\underline{\text{curl}}(\boldsymbol{\eta}) = 0$  in  $\Omega$ , there exists  $C > 0$ , independent of  $h$ , satisfying

$$h_T \|\underline{\text{curl}}(\boldsymbol{\eta}_h)\|_{0,T} \leq C \|\boldsymbol{\eta} - \boldsymbol{\eta}_h\|_{0,T} \quad \text{and} \quad h_e^{1/2} \|\llbracket \gamma_*(\boldsymbol{\eta}_h) \rrbracket\|_{0,e} \leq C \|\boldsymbol{\eta} - \boldsymbol{\eta}_h\|_{0,\omega_e}.$$

Thus, taking  $\boldsymbol{\eta} := \frac{1}{\kappa}(\boldsymbol{\rho} + \theta \mathbf{u}) = \nabla \theta$  and  $\boldsymbol{\eta}_h := \frac{1}{\kappa}(\boldsymbol{\rho}_h + \theta_h \mathbf{u}_h)$ , and using the estimate (5.29) we can obtain (5.35) and (5.36). In turn, these same arguments combined with [21, Lemma 3.26] allows us to deduce the inequality (5.37). Further details are omitted.

On the other hand, the proof for the three-dimensional case follows from a slight modification of the proofs of Lemmas 4.9, 4.10, and 4.13 in [27].  $\square$

We remark that, for simplicity, the derivation of (5.30) in Lemma 5.12 and (5.37) in Lemma 5.13 has required  $\theta_D$  to be piecewise polynomial. However, if  $\theta_D$  is sufficiently smooth, and proceeding similarly as in [12, Section 6.2], higher order terms given by the errors arising from suitable polynomial approximations would appear in (5.30) and (5.37), which explains the eventual h.o.t in (5.22).

We end this section by remarking that the efficiency of  $\Theta$  (cf. (5.22)) in Theorem 5.2 is now a straightforward consequence of Lemmas 5.7 and 5.9–5.13. In turn, we emphasize that the resulting positive constant denoted by  $C_{eff}$  is independent of  $h$ .

## 6 Numerical results

This section serves to illustrate the performance and accuracy of the proposed mixed finite element scheme (3.13) along with the reliability and efficiency properties of the *a posteriori* error estimator  $\Theta$  (cf. (5.1)) derived in Section 5. In what follows, we refer to the corresponding sets of finite elements subspaces generated by  $k = 0$  and  $k = 1$ , as simply  $\mathbb{RT}_0 - \mathbf{P}_0 - \mathbf{RT}_0 - \mathbf{P}_0$  and  $\mathbb{RT}_1 - \mathbf{P}_1 - \mathbf{RT}_1 - \mathbf{P}_1$ , respectively. Our implementation is based on a `FreeFem++` code [30]. Regarding the implementation of the Newton iterative method associated to (3.13) (see [13, Section 6] for details), the iterations are

terminated once the relative error of the entire coefficient vectors between two consecutive iterates, say  $\mathbf{coeff}^m$  and  $\mathbf{coeff}^{m+1}$ , is sufficiently small, i.e.,

$$\frac{\|\mathbf{coeff}^{m+1} - \mathbf{coeff}^m\|_{\ell^2}}{\|\mathbf{coeff}^{m+1}\|_{\ell^2}} \leq \text{tol},$$

where  $\|\cdot\|_{\ell^2}$  is the standard  $\ell^2$ -norm in  $\mathbb{R}^N$ , with  $N$  denoting the total number of degrees of freedom defining the finite element subspaces  $\mathbb{X}_h$ ,  $\mathbf{M}_h$ ,  $\mathbf{H}_h$  and  $\mathbf{Q}_h$  stated in Section 3.3, and  $\text{tol}$  is a fixed tolerance chosen as  $\text{tol} = 1\text{E} - 06$ . As usual, the individual errors are denoted by:

$$\begin{aligned} e(\boldsymbol{\sigma}) &:= \|\boldsymbol{\sigma} - \boldsymbol{\sigma}_h\|_{\mathbb{X}}, & e(\mathbf{u}) &:= \|\mathbf{u} - \mathbf{u}_h\|_{\mathbf{M}}, & e(p) &:= \|p - p_h\|_{0,\Omega}, \\ e(\boldsymbol{\rho}) &:= \|\boldsymbol{\rho} - \boldsymbol{\rho}_h\|_{\mathbf{H}}, & e(\theta) &:= \|\theta - \theta_h\|_{\mathbf{Q}}, \end{aligned}$$

where the pressure  $p$  is approximate through the post-processing formula (cf. [13, eq. (5.16)]):

$$p_h = -\frac{1}{d} \left( \text{tr}(\boldsymbol{\sigma}_h) + \text{tr}(\mathbf{u}_h \otimes \mathbf{u}_h) - \frac{1}{|\Omega|} (\text{tr}(\mathbf{u}_h \otimes \mathbf{u}_h), 1)_{\Omega} \right).$$

We stress here that we are able to recover other variables of physical interest such as the stress tensor, the vorticity, the velocity gradient and the heat-flux vector by a post-processing procedure (see [13, Section 5.3] for details). However, for the sake of simplicity, in the numerical essays below we will focus only on the formula suggested for the pressure field. Then, the global error and the effectivity index associated to the global estimator  $\Theta$  are denoted, respectively, by

$$e(\vec{\mathbf{t}}) := e(\boldsymbol{\sigma}) + e(\mathbf{u}) + e(\boldsymbol{\rho}) + e(\theta) \quad \text{and} \quad \text{eff}(\Theta) := \frac{e(\vec{\mathbf{t}})}{\Theta}.$$

Moreover, using the fact that  $c N^{-1/d} \leq h \leq C N^{-1/d}$ , the experimental rate of convergence of any of the above quantities will be computed as

$$r(\diamond) := -d \frac{\log(e(\diamond)/e'(\diamond))}{\log(N/N')} \quad \text{for each } \diamond \in \{\boldsymbol{\sigma}, \mathbf{u}, \boldsymbol{\rho}, \theta, p, \vec{\mathbf{t}}\},$$

where  $N$  and  $N'$  denote the total degrees of freedom associated to two consecutive triangulations with errors  $e(\diamond)$  and  $e'(\diamond)$ .

The examples to be considered in this section are described next. In all of them, for the sake of simplicity, we consider the thermal conductivity  $\kappa = 1$  and the viscosity of the fluid  $\nu = 1$ . In addition, the condition of zero-average pressure (translated in terms of the trace of  $\boldsymbol{\sigma}_h$ ) is imposed through a real Lagrange multiplier.

Example 1 is used to corroborate the reliability and efficiency of the *a posteriori* error estimator  $\Theta$ , whereas Examples 2 and 3 are utilized to illustrate the behavior of the associated adaptive algorithm in 2D and 3D domains, respectively, which applies the following procedure from [37]:

- (1) Start with a coarse mesh  $\mathcal{T}_h$ .
- (2) Solve the Newton iterative method associated to (3.13) for the current mesh  $\mathcal{T}_h$ .
- (3) Compute the local indicator  $\hat{\Theta}_T$  for each  $T \in \mathcal{T}_h$ , where

$$\hat{\Theta}_T := \Theta_T + \|\theta_h \mathbf{g} + \mathbf{div} \boldsymbol{\sigma}_h\|_{\mathbf{L}^{4/3}(T)} + \|\mathbf{div} \boldsymbol{\rho}_h\|_{\mathbf{L}^{4/3}(T)}, \quad (\text{cf. (5.2)})$$



- (4) Check the stopping criterion and decide whether to finish or go to next step.
- (5) Generate an adapted mesh through a variable metric/Delaunay automatic meshing algorithm (see [31, Section 9.1.9]).
- (6) Define resulting mesh as current mesh  $\mathcal{T}_h$ , and go to step (2).

At this point we mention that, should non-zero source terms appear in the right-hand side of the second equations of (3.3) and (3.4), say  $\mathbf{f}_m$  and  $f_e$ , respectively, some terms in the *a posteriori* error estimator must be modified. More precisely, the quantities

$$\|\theta_h \mathbf{g} + \mathbf{div} \boldsymbol{\sigma}_h\|_{\mathbf{L}^{4/3}(T)} \quad \text{and} \quad \|\mathbf{div} \boldsymbol{\rho}_h\|_{\mathbf{L}^{4/3}(T)}$$

must be replaced by

$$\|\theta_h \mathbf{g} + \mathbf{div} \boldsymbol{\sigma}_h - \mathbf{f}_m\|_{\mathbf{L}^{4/3}(T)} \quad \text{and} \quad \|\mathbf{div} \boldsymbol{\rho}_h - f_e\|_{\mathbf{L}^{4/3}(T)},$$

whose estimation from below and above follows in a straightforward manner.

### Example 1: Accuracy assessment with a smooth solution

In our first example, we concentrate on the accuracy of the mixed method (3.13). The domain is the square  $\Omega = (0, 1) \times (0, 1)$ , the boundary  $\Gamma = \bar{\Gamma}_D \cup \bar{\Gamma}_N$ , with  $\Gamma_N = [0, 1] \times \{1\}$  and  $\Gamma_D = \Gamma \setminus \Gamma_N$ . We consider the external force  $\mathbf{g} = (0, -1)^t$ , and the terms on the right-hand side are adjusted so that a manufactured solution of (3.3)–(3.4) is given by the smooth functions

$$\begin{aligned} \mathbf{u}(x, y) &:= \begin{pmatrix} x^2(x-1)^2 \sin(y) \\ 2x(x-1)(2x-1) \cos(y) \end{pmatrix}, \quad p(x, y) := \cos(\pi x) e^{\pi y} \\ \text{and } \theta(x, y) &:= \frac{1}{2} \sin(\pi x) \cos^2\left(\frac{\pi}{2}(y+1)\right). \end{aligned}$$

Tables 6.1 and 6.2 show the convergence history for a sequence of quasi-uniform mesh refinements, including the average number of Newton iterations. The results illustrate that the optimal rates of convergence  $\mathcal{O}(h)$  and  $\mathcal{O}(h^2)$  provided by Theorem 3.4 are attained for  $k = 0, 1$ . In addition, we also compute the global *a posteriori* error indicator  $\Theta$  (cf. (5.1)), and measure its reliability and efficiency with the effectivity index. Notice that the estimator remain always bounded.

### Example 2: Adaptivity in a 2D L-shape domain

Our second example is aimed at testing the features of adaptive mesh refinement after the *a posteriori* error estimator  $\Theta$  (cf. (5.1)). We consider a L-shape contraction domain  $\Omega := (-1, 1)^2 \setminus (0, 1)^2$ , the boundary  $\Gamma = \bar{\Gamma}_D \cup \bar{\Gamma}_N$ , with  $\Gamma_N = [-1, 0] \times \{1\}$  and  $\Gamma_D = \Gamma \setminus \Gamma_N$ . The external force is chosen as  $\mathbf{g} = (0, -1)^t$ , and the terms on the right-hand side are adjusted so that the exact solution is given by the functions

$$\begin{aligned} \mathbf{u}(x, y) &:= \begin{pmatrix} -\cos(\pi x) \sin(\pi y) \\ \sin(\pi x) \cos(\pi y) \end{pmatrix}, \quad p(x, y) := \frac{1-x}{(x-0.02)^2 + (y-0.02)^2} - p_0 \\ \text{and } \theta(x, y) &:= \frac{1}{y+1.1}, \end{aligned}$$

where  $p_0 \in \mathbb{R}$  is a constant chosen in such a way  $(p, 1)_\Omega = 0$ . Notice that the pressure and temperature exhibit high gradients near the origin and the line  $y = -1.1$ , respectively.

Tables 6.3–6.6 along with Figure 6.1, summarizes the convergence history of the method applied to a sequence of quasi-uniformly and adaptively refined triangulation of the domain. Suboptimal rates are observed in the first case, whereas adaptive refinement according to the *a posteriori* error indicator  $\Theta$  yield optimal convergence and stable effectivity indexes. Notice how the adaptive algorithms improves the efficiency of the method by delivering quality solutions at a lower computational cost, to the point that it is possible to get a better one (in terms of  $e(\tilde{\mathbf{t}})$ ) with approximately only the 1.8% of the degrees of freedom of the last quasi-uniform mesh for the mixed scheme in both cases  $k = 0$  and  $k = 1$ . In addition, and similarly to [10, Remark 4.6], we observe that our Galerkin scheme (3.13) satisfies the properties  $\theta_h \mathbf{g} + \mathbf{div} \boldsymbol{\sigma}_h = \mathbf{P}_h^k(\mathbf{f}_m)$  and  $\text{div} \boldsymbol{\rho}_h = \mathcal{P}_h^k(f_e)$  in  $\Omega$ , where  $\mathcal{P}_h^k$  is the  $L^2(\Omega)$ -orthogonal projection onto discontinuous piecewise polynomials of degree  $k$  and  $\mathbf{P}_h^k$  is its vectorial version. In this way, using the fact that neither  $\mathbf{f}_m$  nor  $f_e$  live in  $\mathbf{M}_h$  and  $\mathbf{Q}_h$  (cf. (3.12)), respectively, we illustrate the conservation of momentum and thermal energy in an approximate sense by computing the  $\ell^\infty$ -norm for  $\mathbf{F}_m := \theta_h \mathbf{g} + \mathbf{div} \boldsymbol{\sigma}_h - \mathbf{P}_h^k(\mathbf{f}_m)$  and  $\mathbf{T}_e := \text{div} \boldsymbol{\rho}_h - \mathcal{P}_h^k(f_e)$ , with  $k = 0, 1$ . As expected, these values are close to zero.

On the other hand, approximate solutions builded using the  $\mathbb{RT}_1 - \mathbf{P}_1 - \mathbf{RT}_1 - \mathbf{P}_1$  scheme with 811,911 degree of freedom (33,717 triangles), via the indicator  $\Theta$ , are shown in Figure 6.3. In particular, we observe that computed pressure and temperature exhibit high gradients near the contraction region and at the bottom boundary of the L-shape domain, respectively. In turn, examples of some adapted meshes generates using  $\Theta$  for  $k = 0$  and  $k = 1$  are collected in Figure 6.2. We can observe a clear clustering of elements around the vertex  $(0, 0)$  and the line  $y = -1.1$ , which illustrate again how the method is able to identify the regions in which the accuracy of the numerical approximation is deteriorated.

### Example 3: Adaptivity in a 3D L-shape domain

Finally, in our third example we turn to the testing of the scheme and the adaptive algorithm in a three-dimensional scenario. More precisely, we consider the 3D L-shape domain  $\Omega := (-0.5, 0.5) \times (0, 0.5) \times (-0.5, 0.5) \setminus (0, 0.5)^3$ , the boundary  $\Gamma = \bar{\Gamma}_D \cup \bar{\Gamma}_N$ , with  $\Gamma_N = \{-0.5\} \times [0, 0.5] \times [-0.5, 0.5]$  and  $\Gamma_D = \Gamma \setminus \Gamma_N$ . We consider the external force  $\mathbf{g} = (0, 0, -1)^t$ , and the terms on the right-hand side are adjusted so that the exact solution is given by the functions

$$\mathbf{u}(x, y, z) := \begin{pmatrix} \sin(\pi x) \cos(\pi y) \cos(\pi z) \\ -2 \cos(\pi x) \sin(\pi y) \cos(\pi z) \\ \cos(\pi x) \cos(\pi y) \sin(\pi z) \end{pmatrix}, \quad p(x, y, z) := \frac{10z}{(x - 0.005)^2 + (y - 0.005)^2} - p_0$$

and  $\theta(x, y, z) := \cos(\pi y) \sin(\pi(x + z)),$

where  $p_0 \in \mathbb{R}$  is a constant chosen in such a way  $(p, 1)_\Omega = 0$ . Notice that the pressure exhibit high gradients near the contraction region of the 3D L-shape domain. The latter is illustrated in Figure 6.4 where the initial mesh and the last two adapted meshes according to the indicator  $\Theta$  for  $k = 0$  show a clear clustering of elements in the contraction region as we expected. Moreover, in Figure 6.5 we compare the exact magnitude of the velocity, the temperature field and the pressure field with their approximate counterparts after four mesh adaptive refinement steps. There we can observe that the approximate solution captures satisfactorily the behavior of the exact solution.

$N$	$e(\sigma)$	$r(\sigma)$	$e(\mathbf{u})$	$r(\mathbf{u})$	$e(\rho)$	$r(\rho)$	$e(\theta)$	$r(\theta)$
294	6.55e+00	—	1.17e-01	—	6.02e-01	—	6.58e-02	—
1173	3.12e+00	1.071	4.44e-02	1.402	2.99e-01	1.011	3.58e-02	0.879
4701	1.50e+00	1.058	1.67e-02	1.411	1.42e-01	1.073	1.59e-02	1.167
18312	7.75e-01	0.970	7.76e-03	1.124	7.01e-02	1.038	7.86e-03	1.040
72729	3.82e-01	1.025	3.92e-03	0.990	3.53e-02	0.993	4.02e-03	0.971
293163	1.91e-01	0.996	1.88e-03	1.053	1.74e-02	1.015	1.97e-03	1.023

$e(p)$	$r(p)$	$e(\vec{\mathbf{t}})$	$r(\vec{\mathbf{t}})$	$\Theta$	$\text{eff}(\Theta)$	iter
1.61e+00	—	7.34e+00	—	1.25e+01	0.586	4
6.83e-01	1.237	3.50e+00	1.069	6.51e+00	0.538	4
2.97e-01	1.202	1.67e+00	1.065	3.37e+00	0.500	4
1.50e-01	1.003	8.61e-01	0.978	1.78e+00	0.483	4
7.09e-02	1.088	4.26e-01	1.021	8.99e-01	0.474	4
3.52e-02	1.006	2.12e-01	0.999	4.61e-01	0.461	4

Table 6.1: EXAMPLE 1:  $\mathbb{RT}_0 - \mathbf{P}_0 - \mathbb{RT}_0 - \mathbf{P}_0$  scheme with quasi-uniform refinement.

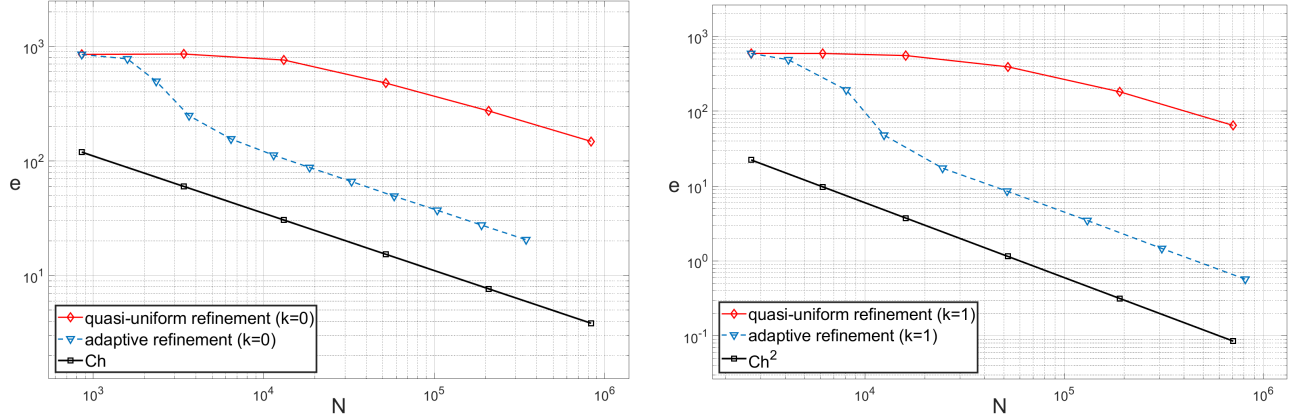


Figure 6.1: EXAMPLE 2: Log-log plot of  $e(\vec{\mathbf{t}})$  vs.  $N$  for quasi-uniform/adaptative refinements for  $k = 0$  and  $k = 1$  (left and right plots, respectively).

## References

- [1] S. AGMON, *Lectures on Elliptic Boundary Value Problems*. Van Nostrand, Princeton, New Jersey, 1965.
- [2] J.A. ALMONACID AND G.N. GATICA, *A fully-mixed finite element method for the  $n$ -dimensional Boussinesq problem with temperature-dependent parameters*. Comput. Methods Appl. Math. 20 (2020), no. 2, 187–213.
- [3] A. ALLENDES, G.R. BARRENECHEA, AND C. NARRANJO, *A divergence-free low-order stabilized finite element method for a generalized steady state Boussinesq problem*. Comput. Methods Appl. Mech. Engrg. 340 (2018), 90–120.
- [4] A. ALLENDES, C. NARANJO, AND E. OTÁROLA. *Stabilized finite element approximations for a generalized Boussinesq problem: A posteriori error analysis*. Comput. Methods Appl. Mech.

$N$	$e(\boldsymbol{\sigma})$	$r(\boldsymbol{\sigma})$	$e(\mathbf{u})$	$r(\mathbf{u})$	$e(\boldsymbol{\rho})$	$r(\boldsymbol{\rho})$	$e(\theta)$	$r(\theta)$
912	7.81e-01	—	1.68e-02	—	7.35e-02	—	8.11e-03	—
2184	3.10e-01	2.117	6.29e-03	2.245	2.86e-02	2.164	2.67e-03	2.546
5880	1.10e-01	2.091	2.27e-03	2.055	1.12e-02	1.889	1.14e-03	1.727
19128	3.26e-02	2.064	6.42e-04	2.143	3.29e-03	2.080	3.01e-04	2.250
65400	9.78e-03	1.957	2.03e-04	1.876	1.01e-03	1.927	9.31e-05	1.910
247320	2.59e-03	1.997	5.28e-05	2.024	2.68e-04	1.989	2.47e-05	1.997

$e(p)$	$r(p)$	$e(\vec{\mathbf{t}})$	$r(\vec{\mathbf{t}})$	$\Theta$	$\text{eff}(\Theta)$	iter
1.42e-01	—	8.79e-01	—	2.62e+00	0.336	4
5.95e-02	1.995	3.47e-01	2.127	1.04e+00	0.333	4
2.13e-02	2.072	1.25e-01	2.070	3.82e-01	0.326	4
6.29e-03	2.070	3.68e-02	2.068	1.15e-01	0.321	4
1.88e-03	1.961	1.11e-02	1.953	3.56e-02	0.312	4
5.04e-04	1.982	2.94e-03	1.997	9.75e-03	0.301	4

Table 6.2: EXAMPLE 1:  $\mathbb{RT}_1 - \mathbf{P}_1 - \mathbf{RT}_1 - \mathbf{P}_1$  scheme with quasi-uniform refinement.

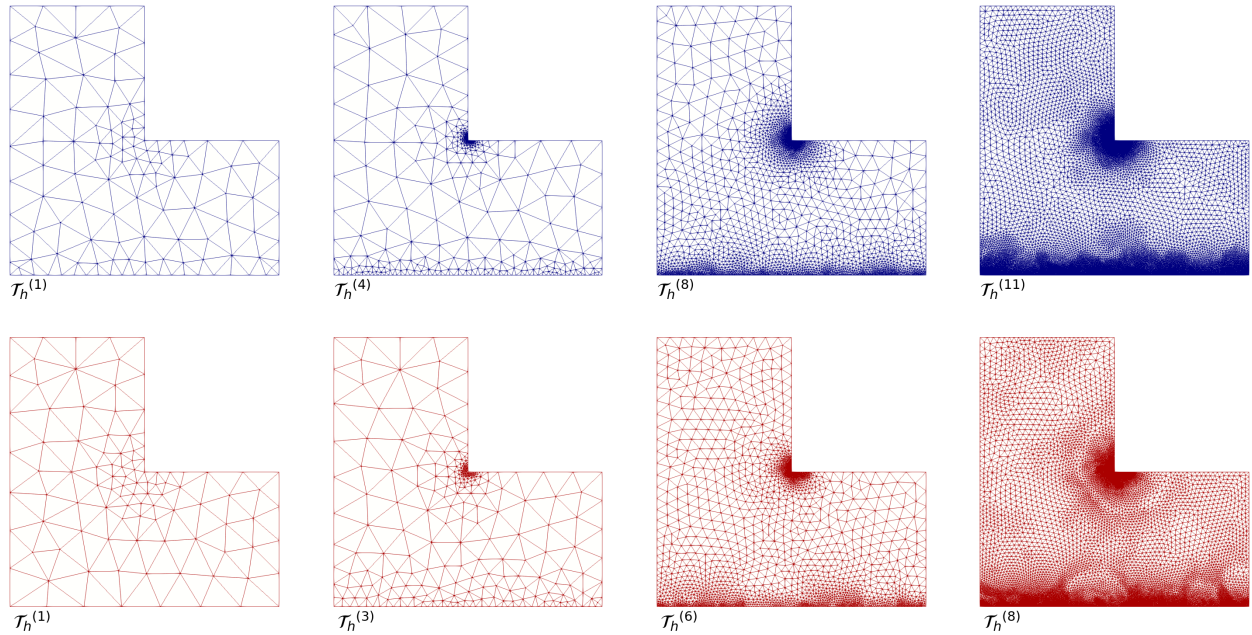


Figure 6.2: EXAMPLE 2: Four snapshots of adapted meshes according to the indicator  $\Theta$  for  $k = 0$  and  $k = 1$  (top and bottom plots, respectively).

Engrg. 361 (2020), 112703, 25 pp.

- [5] M. K. ALLALI, *A priori and a posteriori error estimates for Boussinesq equations*. Int. J. Numer. Anal. Model. 2 (2005), no. 2, 179–196.
- [6] J. ALMONACID, G. GATICA, AND R. OYARZÚA, *A posteriori error analysis of a mixed-primal finite element method for the Boussinesq problem with temperature-dependent viscosity*. J. Sci. Comput. 78 (2019), no. 2, 887–917.

$N$	$e(\boldsymbol{\sigma})$	$r(\boldsymbol{\sigma})$	$e(\mathbf{u})$	$r(\mathbf{u})$	$e(\boldsymbol{\rho})$	$r(\boldsymbol{\rho})$	$e(\theta)$	$r(\theta)$
858	6.72e+02	–	4.77e+00	–	1.72e+02	–	3.10e+00	–
3411	7.38e+02	–	3.46e+00	0.468	1.15e+02	0.583	1.45e+00	1.103
13167	6.91e+02	0.098	2.08e+00	0.752	6.70e+01	0.800	7.15e-01	1.042
52029	4.43e+02	0.648	1.02e+00	1.037	3.46e+01	0.963	3.51e-01	1.035
209343	2.56e+02	0.788	3.50e-01	1.538	1.70e+01	1.023	1.70e-01	1.041
833151	1.39e+02	0.879	1.23e-01	1.516	8.62e+00	0.981	8.66e-02	0.978

$e(p)$	$r(p)$	$e(\vec{\mathbf{t}})$	$r(\vec{\mathbf{t}})$	$\Theta$	$\text{eff}(\Theta)$	$\ \mathbf{F}_m\ _{\ell^\infty}$	$\ \mathbf{T}_e\ _{\ell^\infty}$	iter
3.32e+01	–	8.52e+02	–	1.02e+03	0.836	9.09e-13	2.27e-13	5
3.47e+01	–	8.58e+02	–	1.02e+03	0.841	1.82e-12	4.55e-13	5
2.86e+01	0.284	7.61e+02	0.178	8.95e+02	0.850	3.64e-12	6.82e-13	4
1.75e+01	0.717	4.79e+02	0.674	5.82e+02	0.823	1.46e-11	2.05e-12	4
9.48e+00	0.880	2.73e+02	0.806	3.33e+02	0.820	7.28e-11	4.55e-12	4
5.36e+00	0.824	1.48e+02	0.886	1.83e+02	0.812	1.46e-10	1.23e-11	4

Table 6.3: EXAMPLE 2:  $\mathbf{RT}_0 - \mathbf{P}_0 - \mathbf{RT}_0 - \mathbf{P}_0$  scheme with quasi-uniform refinement.

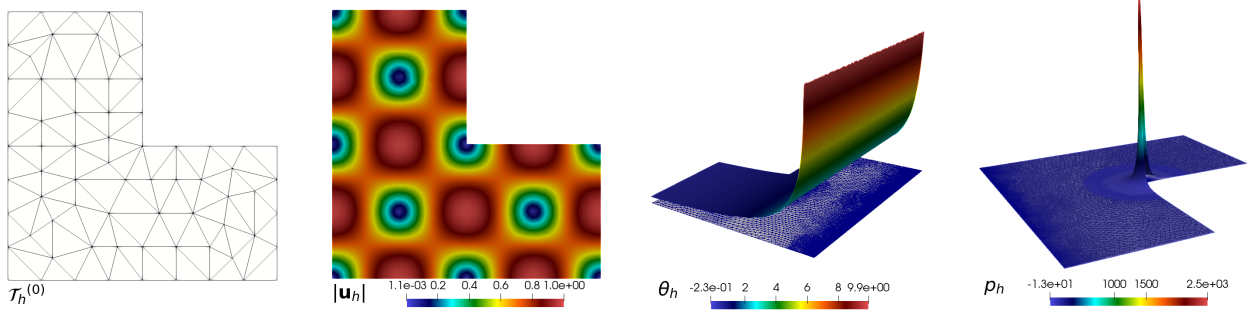


Figure 6.3: EXAMPLE 2: Initial mesh, computed magnitude of the velocity, temperature field and post-processed pressure field (from left to right).

- [7] M. ALVAREZ, G.N. GATICA, AND R. RUIZ-BAIER, *A posteriori error analysis for a viscous flow–transport problem*. ESAIM Math. Model. Numer. Anal. 50 (2016), no. 6, 1789–1816.
- [8] F. BREZZI AND M. FORTIN, *Mixed and Hybrid Finite Element Methods*. Springer Series in Computational Mathematics, 15. Springer-Verlag, New York, 1991.
- [9] J. CAMAÑO, S. CAUCAO, R. OYARZÚA, AND S. VILLA-FUENTES, *A posteriori error analysis of a momentum conservative mixed-FEM for the stationary Navier–Stokes problem*. Preprint 2020-24, Centro de Investigación en Ingeniería Matemática (CI<sup>2</sup>MA), Universidad de Concepción, Concepción, Chile, (2020).
- [10] J. CAMAÑO, C. GARCÍA, AND R. OYARZÚA, *Analysis of a conservative mixed-FEM for the stationary Navier–Stokes problem*. Preprint 2018-25, Centro de Investigación en Ingeniería Matemática (CI<sup>2</sup>MA), Universidad de Concepción, Concepción, Chile, (2018).
- [11] C. CARSTENSEN, *A posteriori error estimate for the mixed finite element method*. Math. Comp. 66 (1997), no. 218, 465–476.

$N$	$e(\boldsymbol{\sigma})$	$r(\boldsymbol{\sigma})$	$e(\mathbf{u})$	$r(\mathbf{u})$	$e(\boldsymbol{\rho})$	$r(\boldsymbol{\rho})$	$e(\theta)$	$r(\theta)$
2688	5.12e+02	–	2.25e+00	–	7.57e+01	–	5.80e-01	–
6144	5.36e+02	–	1.86e+00	0.465	5.21e+01	0.904	3.11e-01	1.509
16080	5.21e+02	0.059	1.31e+00	0.724	3.06e+01	1.106	1.60e-01	1.379
52176	3.79e+02	0.541	4.54e-01	1.801	1.21e+01	1.581	5.86e-02	1.710
190080	1.78e+02	1.168	1.53e-01	1.679	3.40e+00	1.962	1.62e-02	1.984
706704	6.35e+01	1.571	3.40e-02	2.296	9.73e-01	1.905	4.85e-03	1.842

$e(p)$	$r(p)$	$e(\vec{\mathbf{t}})$	$r(\vec{\mathbf{t}})$	$\Theta$	$\text{eff}(\Theta)$	$\ \mathbf{F}_m\ _{\ell^\infty}$	$\ \mathbf{T}_e\ _{\ell^\infty}$	iter
2.11e+01	–	5.90e+02	–	6.85e+03	0.086	9.09e-13	2.27e-13	5
2.01e+01	0.121	5.90e+02	–	4.45e+03	0.132	3.64e-12	6.82e-13	4
1.73e+01	0.303	5.53e+02	0.135	2.06e+03	0.268	1.09e-11	1.82e-12	4
1.06e+01	0.830	3.91e+02	0.587	7.85e+02	0.498	1.46e-11	2.50e-12	4
4.75e+00	1.247	1.82e+02	1.188	4.78e+02	0.380	4.37e-11	6.37e-12	4
1.59e+00	1.663	6.45e+01	1.577	1.64e+02	0.392	1.53e-10	1.75e-11	4

Table 6.4: EXAMPLE 2:  $\mathbb{RT}_1 - \mathbf{P}_1 - \mathbf{RT}_1 - \mathbf{P}_1$  scheme with quasi-uniform refinement.

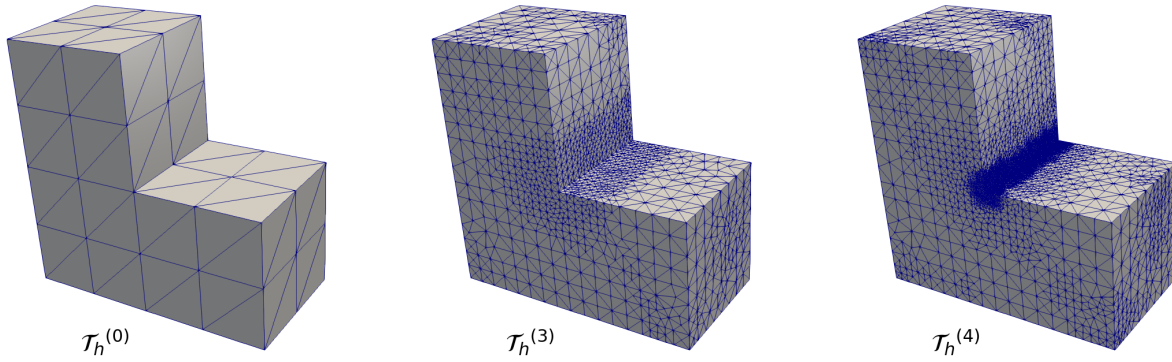


Figure 6.4: EXAMPLE 3: Initial mesh and two snapshots of adapted meshes according to the indicator  $\Theta$  for  $k = 0$  (from left to right).

- [12] S. CAUCAO, D. MORA, AND R. OYARZÚA, *A priori and a posteriori error analysis of a pseudostress-based mixed formulation of the Stokes problem with varying density*. IMA J. Numer. Anal. 36 (2016), no. 2, 947–983.
- [13] S. CAUCAO, R. OYARZÚA, AND S. VILLA-FUENTES, *A new mixed-FEM for steady-state natural convection models allowing conservation of momentum and thermal energy*. Calcolo 57 (2020), no. 4, 36.
- [14] P. CLÉMENT, *Approximation by finite element functions using local regularisation*. RAIRO Modélisation Mathématique et Analyse Numérique 9 (1975), 77–84.
- [15] E. COLMENARES, G.N. GATICA, AND S. MORAGA, *A Banach spaces-based analysis of a new fully-mixed finite element method for the Boussinesq problem*. ESAIM Math. Model. Numer. Anal. 54 (2020), no. 5, 1525–1568.

$N$	$e(\boldsymbol{\sigma})$	$r(\boldsymbol{\sigma})$	$e(\mathbf{u})$	$r(\mathbf{u})$	$e(\boldsymbol{\rho})$	$r(\boldsymbol{\rho})$	$e(\theta)$	$r(\theta)$
858	6.72e+02	—	4.77e+00	—	1.72e+02	—	3.10e+00	—
1494	6.59e+02	0.064	2.29e+00	2.386	1.16e+02	1.274	1.50e+00	2.344
2562	4.01e+02	2.557	7.64e-01	5.633	9.35e+01	1.117	1.10e+00	1.598
4203	1.78e+02	3.674	2.54e-01	4.972	7.01e+01	1.301	7.46e-01	1.758
6627	9.90e+01	2.059	2.47e-01	0.094	5.59e+01	0.796	5.91e-01	0.828
10776	7.61e+01	0.917	2.40e-01	0.111	3.57e+01	1.557	3.67e-01	1.661
17610	5.85e+01	1.083	2.02e-01	0.709	2.88e+01	0.892	2.91e-01	0.956
28650	4.55e+01	0.883	1.39e-01	1.319	2.03e+01	1.230	2.06e-01	1.211
47085	3.30e+01	1.118	1.10e-01	0.795	1.60e+01	0.828	1.58e-01	0.928
77445	2.58e+01	0.850	7.26e-02	1.440	1.12e+01	1.232	1.12e-01	1.170
124623	1.88e+01	1.050	5.67e-02	0.830	8.58e+00	0.886	8.44e-02	0.957
200520	1.45e+01	0.877	3.66e-02	1.449	6.00e+00	1.191	5.97e-02	1.151

$e(p)$	$r(p)$	$e(\vec{\mathbf{t}})$	$r(\vec{\mathbf{t}})$	$\Theta$	$\text{eff}(\Theta)$	$\ \mathbf{F}_{\mathbf{m}}\ _{\ell^\infty}$	$\ \mathbf{T}_{\mathbf{e}}\ _{\ell^\infty}$	iter
3.32e+01	—	8.52e+02	—	1.02e+03	0.836	9.09e-13	2.27e-13	5
2.64e+01	0.744	7.79e+02	0.291	9.24e+02	0.842	3.64e-12	4.55e-13	5
1.46e+01	3.047	4.96e+02	2.320	5.90e+02	0.841	1.46e-11	6.82e-13	4
6.29e+00	3.799	2.49e+02	3.118	2.96e+02	0.839	6.18e-11	1.14e-12	4
3.72e+00	1.857	1.56e+02	1.649	1.89e+02	0.826	3.75e-10	2.05e-12	4
2.80e+00	0.989	1.12e+02	1.135	1.36e+02	0.827	7.75e-10	3.41e-12	4
2.16e+00	1.064	8.78e+01	1.020	1.06e+02	0.824	9.02e-10	5.46e-12	4
1.66e+00	0.917	6.62e+01	0.995	8.03e+01	0.824	1.63e-09	7.28e-12	4
1.20e+00	1.149	4.93e+01	1.025	6.00e+01	0.821	1.80e-09	8.64e-12	4
9.33e-01	0.857	3.71e+01	0.972	4.53e+01	0.819	3.09e-09	1.57e-11	4
6.82e-01	1.047	2.76e+01	0.999	3.38e+01	0.814	3.71e-09	1.77e-11	4
5.22e-01	0.890	2.06e+01	0.974	2.53e+01	0.811	6.47e-09	2.98e-11	4

Table 6.5: EXAMPLE 2:  $\mathbb{RT}_0 - \mathbf{P}_0 - \mathbf{RT}_0 - \mathbf{P}_0$  scheme with adaptive refinement via  $\Theta$ .

- [16] E. COLMENARES, G.N. GATICA, AND R. OYARZÚA, *Analysis of an augmented mixed-primal formulation for the stationary Boussinesq problem*. Numer. Methods Partial Differential Equations 32 (2016), no. 2, 445–478.
- [17] E. COLMENARES, G.N. GATICA, AND R. OYARZÚA, *A posteriori error analysis of an augmented fully-mixed formulation for the stationary Boussinesq model*. Comput. Math. Appl. 77 (2019), no. 3, 693–714.
- [18] E. COLMENARES AND M. NEILAN, *Dual-mixed finite element methods for the stationary Boussinesq problem*. Comput. Math. Appl. 72 (2016), no. 7, 1828–1850.
- [19] E. COLMENARES, G.N. GATICA, AND R. OYARZÚA, *An augmented fully-mixed finite element method for the stationary Boussinesq problem*. Calcolo 54 (2017), no. 1, 167–205.
- [20] E. COLMENARES, G.N. GATICA, AND R. OYARZÚA, *A posteriori error analysis of an augmented mixed-primal formulation for the stationary Boussinesq model*. Calcolo 54 (2017), no. 3, 1055–1095.



$N$	$e(\boldsymbol{\sigma})$	$r(\boldsymbol{\sigma})$	$e(\mathbf{u})$	$r(\mathbf{u})$	$e(\boldsymbol{\rho})$	$r(\boldsymbol{\rho})$	$e(\theta)$	$r(\theta)$
2688	5.12e+02	—	2.25e+00	—	7.57e+01	—	5.80e-01	—
4134	4.09e+02	1.043	7.63e-01	5.022	7.59e+01	—	5.72e-01	0.069
8067	1.65e+02	2.713	1.09e-01	5.812	2.69e+01	3.101	1.41e-01	4.193
12489	3.22e+01	7.477	2.88e-02	6.105	1.55e+01	2.512	7.63e-02	2.801
24567	1.15e+01	3.050	2.71e-02	0.184	5.78e+00	2.926	2.98e-02	2.782
51774	5.17e+00	2.139	2.60e-02	0.110	3.33e+00	1.478	1.82e-02	1.323
130833	2.29e+00	1.754	3.50e-03	4.326	1.16e+00	2.269	6.19e-03	2.327
309630	8.81e-01	2.223	3.33e-03	0.112	5.80e-01	1.617	2.84e-03	1.811
811911	3.84e-01	1.724	5.75e-04	3.644	1.86e-01	2.363	9.87e-04	2.190

$e(p)$	$r(p)$	$e(\vec{\mathbf{t}})$	$r(\vec{\mathbf{t}})$	$\Theta$	$\text{eff}(\Theta)$	$\ \mathbf{F}_m\ _{\ell^\infty}$	$\ \mathbf{T}_e\ _{\ell^\infty}$	iter
2.11e+01	—	5.90e+02	—	6.85e+03	0.086	9.09e-13	2.27e-13	5
8.81e+00	4.055	4.86e+02	0.902	1.51e+03	0.322	3.64e-12	3.41e-13	4
4.11e+00	2.280	1.92e+02	2.775	5.69e+02	0.338	8.73e-11	1.36e-12	4
7.66e-01	7.692	4.79e+01	6.362	1.32e+02	0.363	1.75e-10	2.27e-12	4
3.23e-01	2.554	1.73e+01	3.006	4.68e+01	0.370	8.15e-10	7.28e-12	4
1.38e-01	2.274	8.55e+00	1.894	2.33e+01	0.367	2.71e-09	1.46e-11	4
6.25e-02	1.711	3.47e+00	1.947	9.19e+00	0.377	3.06e-09	2.27e-11	4
2.31e-02	2.308	1.47e+00	1.998	3.98e+00	0.368	8.79e-09	2.68e-11	4
1.03e-02	1.671	5.71e-01	1.958	1.51e+00	0.379	1.05e-08	6.41e-11	4

Table 6.6: EXAMPLE 2:  $\mathbb{RT}_1 - \mathbf{P}_1 - \mathbf{RT}_1 - \mathbf{P}_1$  scheme with adaptive refinement via  $\Theta$ .

- [21] C. DOMÍNGUEZ, G.N. GATICA, AND S. MEDDAHI, *A posteriori error analysis of a fully-mixed finite element method for a two-dimensional fluid-solid interaction problem*. J. Comput. Math. 33 (2015), no. 6, 606–641.
- [22] A. ERN AND J.-L. GUERMOND, *Theory and Practice of Finite Elements*. Applied Mathematical Sciences, 159. Springer-Verlag, New York, 2004.
- [23] M. FARHLOUL, S. NICAISE, AND L. PAQUET *A mixed formulation of Boussinesq equations: analysis of nonsingular solutions*. Math. Comp. 69 (2000), no. 231, 965–986.
- [24] M. FARHLOUL, S. NICAISE, AND L. PAQUET, *A refined mixed finite element method for the Boussinesq equations in polygonal domains*. IMA J. Numer. Anal. 21 (2001), no. 2, 525–551.
- [25] G.N. GATICA, *A note on stable Helmholtz decompositions in 3D*. Appl. Anal. vol 99, no. 7, 1110–1121, (2020).
- [26] G.N. GATICA, *A Simple Introduction to the Mixed Finite Element Method. Theory and applications*. SpringerBriefs in Mathematics. Springer, Cham, 2014.
- [27] G.N. GATICA, L.F. GATICA, AND F.A. SEQUEIRA, *A priori and a posteriori error analyses of a pseudostress-based mixed formulation for linear elasticity*. Comput. Math. Appl. 71 (2016), no. 2, 585–614.
- [28] V. GIRAULT AND P.-A. RAVIART, *Finite Element Methods for Navier–Stokes Equations. Theory and Algorithms*. Springer Series in Computational Mathematics, 5. Springer-Verlag, Berlin, 1986.



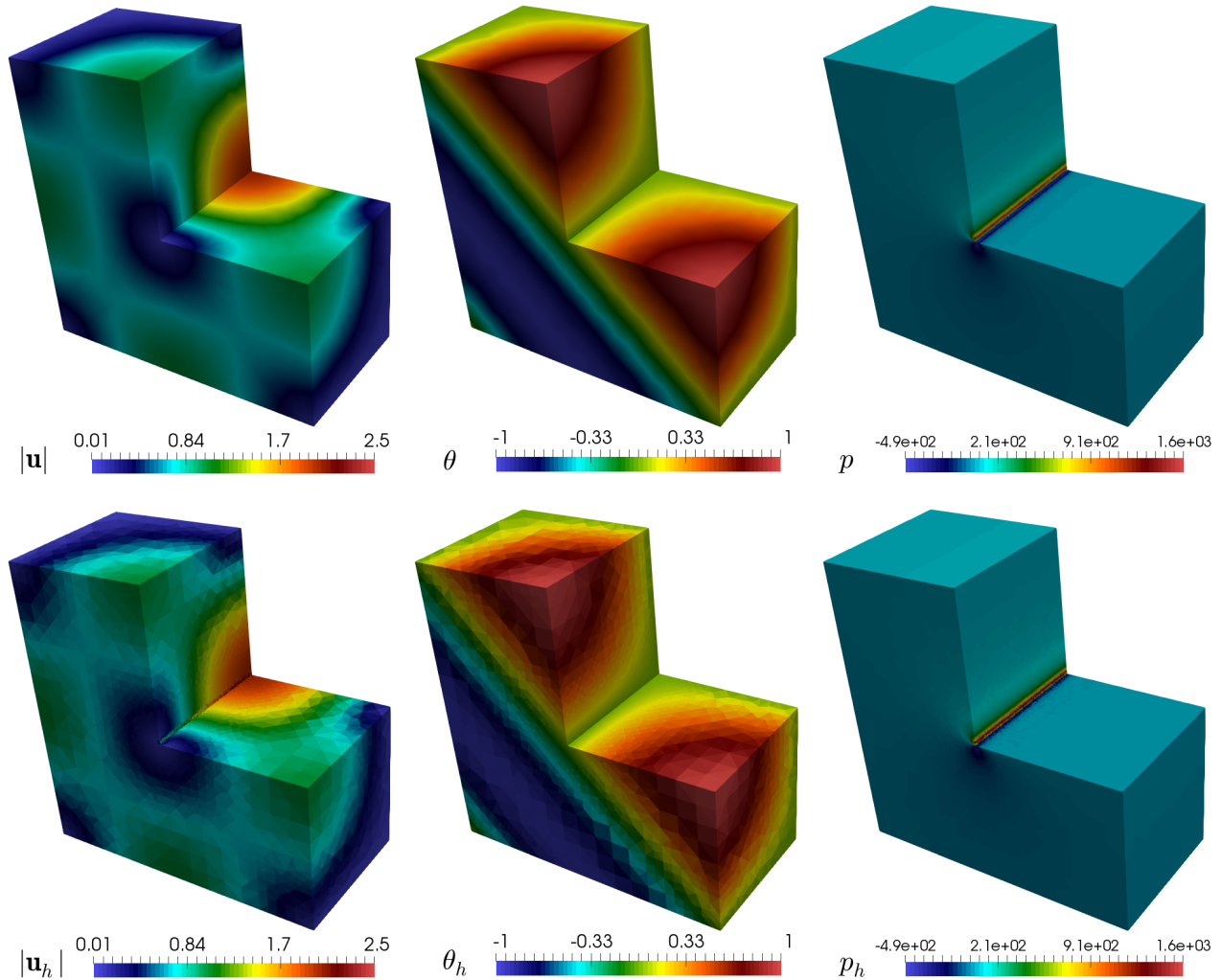


Figure 6.5: EXAMPLE 3: Exact (top plots) and approximate (bottom plots) magnitude of the velocity, temperature field, and pressure field.

- [29] Z. GUO, J. SU, H. CHEN, AND X. LIU, *An adaptive finite element method for stationary incompressible thermal flow based on projection error estimation*. Math. Probl. Eng. 2013 (2013), 14 pages.
- [30] F. HECHT, *New development in freefem++*. J. Numer. Math. 20 (2012), no. 3-4, 251–265.
- [31] F. HECHT, *Freefem++*. Third Edition, Version 3.58-1. Laboratoire Jacques-Louis Lions, Université Pierre et Marie Curie, Paris, 2018. [available in <http://www.freefem.org/ff++>].
- [32] R. OYARZÚA, T. QIN, AND D. SCHÖTZAU, *An exactly divergence-free finite element method for a generalized Boussinesq problem*. IMA J. Numer. Anal. 34 (2014), no. 3, 1104–1135.
- [33] R. OYARZÚA AND M. SERÓN, *A divergence-conforming DG-mixed finite element method for the stationary Boussinesq problem*. J. Sci. Comput. 85 (2020), no. 1, Paper No. 14, 36 pp.
- [34] R. OYARZÚA AND P. ZÚÑIGA, *Analysis of a conforming finite element method for the Boussinesq problem with temperature-dependent parameters*. J. Comput. Appl. Math. 323 (2017), 71–94.

- [35] T. JAKAB, I. MITREA, AND M. MITREA, *Sobolev estimates for the Green potential associated with the Robin-Laplacian in Lipschitz domains satisfying a uniform exterior ball condition, Sobolev Spaces in mathematics II, Applications in Analysis and Partial Differential Equations*. International Mathematical Series, Vol. 9. Springer, Novosibirsk, 2008.
- [36] R. VERFÜRTH, *A posteriori error estimation and adaptive mesh-refinement techniques*. J. Comput. Appl. Math. 50 (1994), no. 1-3, 67–83.
- [37] R. VERFÜRTH, *A Review of A-Posteriori Error Estimation and Adaptive Mesh-Refinement Techniques*. Wiley Teubner, Chichester, 1996.
- [38] Y. ZHANG, Y. HOU, AND H. ZUO, *A posteriori error estimation and adaptive computation of conduction convection problems*. Appl. Math. Model. 35 (2011), 2336–2347.

# Centro de Investigación en Ingeniería Matemática (CI<sup>2</sup>MA)

## PRE-PUBLICACIONES 2020

- 2020-18 DAVID MORA, IVÁN VELÁSQUEZ: *Virtual elements for the transmission eigenvalue problem on polytopal meshes*
- 2020-19 GABRIEL N. GATICA, GEORGE C. HSIAO, SALIM MEDDAHI: *Further developments on boundary-field equation methods for nonlinear transmission problems*
- 2020-20 NICOLAS BARNAFI, GABRIEL N. GATICA, DANIEL E. HURTADO, WILLIAN MIRANDA, RICARDO RUIZ-BAIER: *New primal and dual-mixed finite element methods for stable image registration with singular regularization*
- 2020-21 GONZALO A. BENAVIDES, SERGIO CAUCAO, GABRIEL N. GATICA, ALEJANDRO A. HOPPER: *A new non-augmented and momentum-conserving fully-mixed finite element method for a coupled flow-transport problem*
- 2020-22 RAIMUND BÜRGER, ELVIS GAVILÁN, DANIEL INZUNZA, PEP MULET, LUIS M. VILLADA: *Exploring a convection-diffusion-reaction model of the propagation of forest fires: computation of risk maps for heterogeneous environments*
- 2020-23 GABRIEL N. GATICA, RICARDO OYARZÚA, RICARDO RUIZ-BAIER, YURI D. SOBRAL: *Banach spaces-based analysis of a fully-mixed finite element method for the steady-state model of fluidized beds*
- 2020-24 JESSIKA CAMAÑO, SERGIO CAUCAO, RICARDO OYARZÚA, SEGUNDO VILLA-FUENTES: *A posteriori error analysis of a momentum conservative Banach-spaces based mixed-FEM for the Navier-Stokes problem*
- 2020-25 RAIMUND BÜRGER, JULIO CAREAGA, STEFAN DIEHL: *A method-of-lines formulation for a model of reactive settling in tanks with varying cross-sectional area*
- 2020-26 RAIMUND BÜRGER, CHRISTOPHE CHALONS, RAFAEL ORDOÑEZ, LUIS M. VILLADA: *A multiclass Lighthill-Whitham-Richards traffic model with a discontinuous velocity function*
- 2020-27 TOMÁS BARRIOS, EDWIN BEHRENS, ROMMEL BUSTINZA: *An a posteriori error estimate for a dual mixed method applied to Stokes system with non null source terms*
- 2020-28 RODOLFO ARAYA, CRISTIAN CÁRCAMO, ABNER POZA: *An adaptive stabilized finite element method for the Darcy's equations with pressure dependent viscosities*
- 2020-29 SERGIO CAUCAO, RICARDO OYARZÚA, SEGUNDO VILLA-FUENTES: *A posteriori error analysis of a momentum and thermal energy conservative mixed-FEM for the Boussinesq equations*

Para obtener copias de las Pre-Publicaciones, escribir o llamar a: DIRECTOR, CENTRO DE INVESTIGACIÓN EN INGENIERÍA MATEMÁTICA, UNIVERSIDAD DE CONCEPCIÓN, CASILLA 160-C, CONCEPCIÓN, CHILE, TEL.: 41-2661324, o bien, visitar la página web del centro: <http://www.ci2ma.udec.cl>



**CENTRO DE INVESTIGACIÓN EN  
INGENIERÍA MATEMÁTICA (CI<sup>2</sup>MA)  
Universidad de Concepción**



Casilla 160-C, Concepción, Chile  
Tel.: 56-41-2661324/2661554/2661316  
<http://www.ci2ma.udec.cl>

